

**THE**  
***NMR***  
**NEWSLETTER**

**No. 447**  
**December 1995**

---

<sup>27</sup> Al MAS NMR at 17.6T . . . . .	<b>Kennedy, G. J.</b>	<b>2</b>
Revisiting the INEPT Pulse Sequence and <sup>29</sup> Si NMR Identification of Initial Condensation Products in Organoalkoxysilanes . . . . .	<b>Alam, T. M., and Assink, R. A.</b>	<b>5</b>
Molecular Dynamics of Sodium <i>n</i> -Alkylbenzenesulfonate Adsorbed onto Alumina . . . . .	<b>Nagashima, K., and Blum, F. D.</b>	<b>7</b>
NMR with Electronically Conductive Samples . . . . .	<b>Reimer, J. A., and Yahnke, M. S.</b>	<b>11</b>
Decoupler Problem or New Decoupler Test? . . . . .	<b>Mainz, V. V., and Molitor, P.</b>	<b>15</b>
From Spectral Editing to Extracting Dipolar Couplings in Partially Oriented Systems . . . . .	<b>Ramanathan, K. V., and Khetrapal, C. L.</b>	<b>19</b>
Multislice <sup>1</sup> H Magnetic Resonance Spectroscopic Imaging to Study Dementia . . . . .	<b>Schuff, N., Haupt, C. I., Weiner, M. W., and Maudsley, A. A.</b>	<b>23</b>
Non-Selective T <sub>1</sub> Relaxation Time Measurements by the Newly Developed IR-TOCSY . . . . .	<b>Huber, J. G., and Gaillard, J.</b>	<b>27</b>
Pure-Phase Selective Excitation . . . . .	<b>Caldarelli, S.</b>	<b>31</b>
Field of Dreams, I. Installation Nightmare #32 . . . . .	<b>Shaffer, K.</b>	<b>32</b>
Magnetic Field Dependence of Water Proton Transverse Relaxation in Gelatin . . . . .	<b>Traore, A., Foucat, L., and Renou, J. P.</b>	<b>35</b>
Correction for Intensities of Partially Relaxed NOESY Experiments . . . . .	<b>Liu, H., Tonelli, M., and James, T. L.</b>	<b>39</b>

A monthly collection of informal private letters from laboratories involved with NMR spectroscopy. Information contained herein is solely for the use of the reader. Quotation of material from the Newsletter is not permitted, except by direct arrangement with the author of the letter, in which case the material quoted must be referred to as a "Private Communication". Results, findings, and opinions appearing in the Newsletter are solely the responsibility of the author(s). Reference to The NMR Newsletter or its previous names in the open literature is strictly forbidden.

These restrictions and policies apply equally to both the actual Newsletter recipient/participants and to all others who are allowed access to the Newsletter issues. Strict adherence to this policy is considered essential to the successful continuation of the Newsletter as an informal medium for the exchange of NMR-related information.





## AGILE FREQUENCY GENERATORS-DIRECT SYNTHESIZERS

Accurate, stable frequencies on command, fast switching. For NMR, SATCOM, Surveillance, ATE, Laser, Fluorescence, Clock Sources. Low noise/jitter. Sources adapting to your needs with options. High demonstrated reliability. 20,000+ delivered in 20 years.

	Frequency Range	Resolution	Switching Time <sup>1</sup>	Phase-Continuous Switching <sup>2</sup>	Rack-Mount Cabinet Dim. <sup>3</sup>	Remote-Control Interface	Price Example <sup>4</sup>
PTS 040	.1-40 MHz	optional .1 Hz to 100 KHz	1-20 $\mu$ s	optional	5¼"H×19"W	BCD (std) or GPIO (opt)	\$5,330.00 (1 Hz resol., OCXO freq. std.)
PTS 120	90-120 MHz	optional .1 Hz to 100 KHz	1-20 $\mu$ s	optional	5¼"H×19"W	BCD (std) or GPIO (opt)	\$5,330.00 (1 Hz resol., OCXO freq. std.)
PTS 160	.1-160 MHz	optional .1 Hz to 100 KHz	1-20 $\mu$ s	optional	5¼"H×19"W	BCD (std) or GPIO (opt)	\$6,495.00 (1 Hz resol., OCXO freq. std.)
PTS 250	1-250 MHz	optional .1 Hz to 100 KHz	1-20 $\mu$ s	optional	5¼"H×19"W	BCD (std) or GPIO (opt)	\$7,440.00 (1 Hz resol., OCXO freq. std.)
Type 1 PTS 310	.1-310 MHz	1 Hz	1-20 $\mu$ s	standard	3½"H×19"W	BCD (std) or GPIO (opt)	1 Hz resol., OCXO: \$6,425.00
Type 2							1 Hz resol., OCXO: \$5,850.00
PTS 500	1-500 MHz	optional .1 Hz to 100 KHz	1-20 $\mu$ s	optional	5¼"H×19"W	BCD (std) or GPIO (opt)	\$8,720.00 (1 Hz resol., OCXO freq. std.)
PTS 620	1-620 MHz	optional .1 Hz to 100 KHz	1-20 $\mu$ s	optional	5¼"H×19"W	BCD (std) or GPIO (opt)	\$9,625.00 (1 Hz resol., OCXO freq. std.)
PTS 1000	0.1-1000 MHz	optional .1 Hz to 100 KHz	5-10 $\mu$ s	optional	5¼"H×19"W	BCD (std) or GPIO (opt)	\$11,830.00 (1 Hz resol., OCXO freq. std.)
PTS 3200	1-3200 MHz	1 Hz	1-20 $\mu$ s	optional	5¼"H×19"W	BCD (std) or GPIO (opt)	\$14,850.00 (1 Hz resol., OCXO freq. std.)
PTS x10	user specified 10 MHz decade	1 Hz	1-5 $\mu$ s	standard	3½"H×19"W	BCD (std) or GPIO (opt)	\$3,000.00 (1 Hz resol., OCXO freq. std.)
PTS D310	two channels .1-310 MHz	.1 Hz	1-20 $\mu$ s	standard	5¼"H×19"W	BCD (std) or GPIO (opt)	\$8,560.00 (.1 Hz resol., OCXO freq. std.)
PTS D620	two channels 1-620 MHz	.1 Hz/.2 Hz	1-20 $\mu$ s	standard	5¼"H×19"W	BCD (std) or GPIO (opt)	\$13,240.00 (.1 Hz/.2 Hz resol., OCXO freq. std.)



1 Switching Time is dependent on digit (decade) switched; see detailed instrument specifications.

2 For applicable digits, see detailed instrument specifications.

3 Bench cabinets are 17" wide.

4 Prices are U.S. only and include Manual and Remote (BCD) Control; PTS 3200 Digital Front Panel.

# PROGRAMMED TEST SOURCES, INC.

P.O. Box 517, 9 Beaver Brook Rd., Littleton, MA 01460 Tel: 508-486-3400 FAX: 508-486-4405

THE NMR NEWSLETTER		NO. 447, DECEMBER 1995		AUTHOR INDEX			
Alam, T. M. . . . .	5	Huber, J. G. . . . .	27	Maudsley, A. A. . . . .	23	Schuff, N. . . . .	23
Assink, R. A. . . . .	5	James, T. L. . . . .	39	Molitor, P. . . . .	15	Shaffer, K. . . . .	32
Blum, F. D. . . . .	7	Kennedy, G. J. . . . .	2	Nagashima, K. . . . .	7	Tonelli, M. . . . .	39
Caldarelli, S. . . . .	31	Khetrapal, C. L. . . . .	19	Ramanathan, K. V. . . . .	19	Traore, A. . . . .	35
Foucat, L. . . . .	35	Liu, H. . . . .	39	Reimer, J. A. . . . .	11	Weiner, M. W. . . . .	23
Gaillard, J. . . . .	27	Mainz, V. V. . . . .	15	Renou, J. P. . . . .	35	Yahnke, M. S. . . . .	11
Haupt, C. I. . . . .	23						

THE NMR NEWSLETTER		NO. 447, DECEMBER 1995	ADVERTISER INDEX
American Microwave Technology. . . . .	13	Isotec Inc. . . . .	separate
Bruker Instruments, Inc. . . . .	3, 25	JEOL . . . . .	outside back cover
Cambridge Isotope Laboratories . . . . .	29	Oxford Instruments, Ltd . . . . .	21
Chemagnetics/Otsuka. . . . .	17	Programmed Test Sources, Inc. . . . .	inside front cover
Global Solutions, Inc . . . . .	37	Varian . . . . .	9
International Equipment Trading, Ltd. . . . .	33		

#### SPONSORS OF THE NMR NEWSLETTER

Abbott Laboratories  
Aldrich Chemical Company, Inc.  
American Microwave Technology  
Amgen, Inc.  
Bruker Instruments, Inc.  
Cryomag Services, Inc.  
The Dow Chemical Company  
Eastman Kodak Company  
E. I. du Pont de Nemours & Company  
Hewlett-Packard Company  
Isotec, Inc.  
JEOL (U.S.A.) Inc., Analytical Instruments Division

The Lilly Research Laboratories, Eli Lilly & Company  
Nalorac Cryogenics Corporation  
Otsuka Electronics USA Inc.  
Oxford Instruments  
Programmed Test Sources, Inc.  
SINTEF Unimed MR Center, Trondheim, Norway  
Tecmag  
Unilever Research  
Union Carbide Corporation  
The Upjohn Company  
Varian, Analytical Instrument Division

#### FORTHCOMING NMR MEETINGS

**37th ENC (Experimental NMR Conference)**, Asilomar Conference Center, Pacific Grove, California, **March 17 - 22, 1996**; Contact: ENC, 1201 Don Diego Avenue, Santa Fe, NM 87501; (505) 989-4573; Fax: (505) 989-1073.

**Society of Magnetic Resonance, Fourth Scientific Meeting and Exhibition**, New York, NY, **April 27 - May 3, 1996**; Contact: SMR Office, 2118 Milvia St., Suite 201, Berkeley, CA 94704; (510) 841-1899; Fax: (541) 841-2340. E-mail: info@smr.org. Future meetings: 1997, April 12-18, Vancouver, BC, Canada; 1998, April 18-24, Sydney, Australia; 1999, Philadelphia, PA; 2000, Denver, CO.

**NMR Symposium at the 38th Rocky Mountain Conference on Analytical Chemistry**, Denver, Colorado, **July 22-25, 1996**; Contact: Dr. Joel R. Garbow, Monsanto Company, 700 Chesterfield Parkway North, St. Louis, MO 63198; (314) 537-6004; Fax: (314) 537-6806; e-mail: jrgarb@snc.monsanto.com; See Newsletter **445**, 48.

**XVIIth International Conference on Magnetic Resonance in Biological Systems**, Keystone, Colorado, **August 18 - 23, 1996**; Contact: ICMRBS, 1201 Don Diego Avenue, Santa Fe, NM 87501; (505) 989-4735; Fax: (505) 989-1073.

**38th ENC (Experimental NMR Conference)**, Orlando, FL, **March 23 - 27, 1997**; Contact: ENC, 1201 Don Diego Avenue, Santa Fe, NM 87501; (505) 989-4573; Fax: (505) 989-1073.

Additional listings of meetings, etc., are invited.

# Mobil Research and Development Corporation

PAULSBORO RESEARCH LABORATORY  
P.O. BOX 480  
PAULSBORO, NEW JERSEY 08066-0480

October 10, 1995  
(received 11/4/95)

Dr. B. L. Shapiro  
The NMR Newsletter  
966 Elsinore Court  
Palo Alto, CA 94303

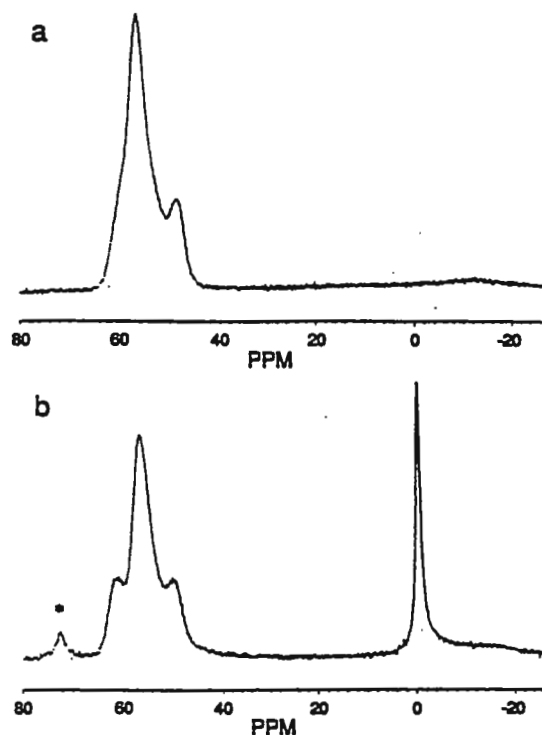
## *<sup>27</sup>Al MAS NMR AT 17.6 T*

Theory tells us and experience has shown that high-resolution solid-state NMR spectra of many inorganic materials can be obtained at high magnetic fields on conventional high-resolution NMR spectrometers by employing magic angle spinning alone. In fact, this recognition of the magnetic field dependence on the NMR spectra of important nuclei such as <sup>27</sup>Al was probably the most important factor in the purchase of our Bruker AM-500 NMR (11.7T) spectrometer over a decade ago. At that time the highest available stable magnetic field available for use with commercial NMR instruments was 11.7T (500MHz for <sup>1</sup>H). Since that time significant technological advances resulted in the commercialization of systems with 14.1T magnets (600MHz for <sup>1</sup>H), and more recently with 17.6T magnets (750MHz for <sup>1</sup>H). As part of our continuing effort to evaluate the potential impact of new NMR technology on our characterization programs, Dr. Stefan Steuernagel of Bruker Instruments graciously agreed to record <sup>27</sup>Al MAS NMR data on a representative group of samples on a 17.6T NMR instrument. In this contribution an example of these very high field NMR data are presented.

The 17.6T <sup>27</sup>Al MAS NMR spectra of zeolite MCM-22 before and after calcination to remove the organic directing agent are shown in the accompanying figure. These data show that there are at least three tetrahedral (T<sub>d</sub>) resonances in the spectrum of MCM-22. The <sup>27</sup>Al MAS NMR spectra of framework aluminosilicates usually consist of one resonance in the 54-68 ppm region of the spectrum that reflects the average environment of an Al atom in the tetrahedral framework. The observation of more than one T<sub>d</sub> resonance for a zeolite is rare. Zeolites omega and ZSM-18 are the only reported cases of zeolites that exhibit two T<sub>d</sub> resonances. Multifield MAS and DOR NMR experiments show that there are no significant second order quadrupolar interactions present and that the multiple T<sub>d</sub> Al resonances are due to distinct T<sub>d</sub> sites in the framework of MCM-22. A discussion of how these unique spectral features relate to the proposed structure of MCM-22 and the nature of the calcination induced changes will be published in the near future.

Best regards,

*Gordon Kennedy*  
Gordon J. Kennedy



<sup>27</sup>Al MAS NMR spectra of MCM-22 before (a) and after (b) calcination. \* denotes sideband from O<sub>h</sub> peak at 0.0 ppm.



*Re*  
The NMR evolution advances...



# XWIN-NMR™ Software:

On-line help is just a click away!



Bruker's new NMR software package, *XWIN-NMR™*, comes complete with an **on-line** manual. *XWIN-NMR™* uses the Frame-Viewer utility to display the manual. Additionally, the table of contents and a keyword index for the manual are organized as hypertext for fast display of a desired item. Now "help" is just a click away!





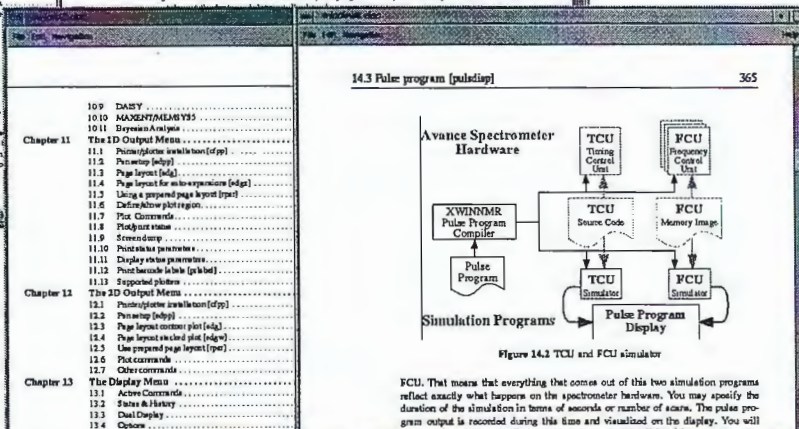
# ...The NMR evolution advances

Contents	
Chapter 1	Introduction
1.1	Hardware and software requirements
1.2	Installation and start-up of XWIN-NMR
1.3	Navigation
1.4	Variables
1.5	XWIN-NMR screen layout
1.6	Manipulation of the XWIN-NMR window
Chapter 2	1D Data Processing Tutorial
2.1	Getting the data set
2.2	Manipulating the data set
2.3	Setting the size of the real spectrum
2.4	Applying a window function to the data
2.5	Applying the Fourier Transform
2.6	Phase correction
2.7	Spectrum calibration
2.8	Baseline correction
2.9	Spectrum integration
2.10	Peak picking
2.11	Plotting
Chapter 3	2D Data Processing Tutorial
3.1	Getting the data set
3.2	Manipulating the spectrum on the screen
3.3	Setting up the parameters for a 2D transform
3.4	Applying the 2D Fourier Transform
3.5	Step and other transforms, and line
3.6	Phase correction
3.7	Spectrum calibration
3.8	Baseline correction
3.9	Spectrum integration
3.10	Spectrum integration
3.11	Peak picking
3.12	Plotting
3.13	Projection and Cross Section
Chapter 4	3D Data Processing Tutorial
4.1	Getting the data set
4.2	Manipulating the spectrum on the screen
4.3	Setting up the parameters for a 3D transform
4.4	Applying the 3D Fourier Transform
4.5	Step transforms, linear projections, and
4.6	Phase correction

## Chapter 3 2D Data Processing Tutorial

This chapter presents 2D data processing based on the data set *exm02d*. The data set is stored in the directory *data\exm02d\exm02d*. In order to have full access permissions to it, you should have a user profile installed on your system, and be logged in as *guest*. Start XWIN-NMR by typing *exm02d* at the prompt. The *-r* option ensures that everything is cleaned up before starting the program, even if the last session was terminated by some problem. The program will start without displaying a data set. Instead, the XWIN-NMR logo will be shown in the data area. In later sections, you can start XWIN-NMR without specifying the *-r* option, and you will immedi-

Here are some pages from the on-line manual, showing the Table of Contents that was used to find the page.



FCU. That means that everything that comes out of this two simulation programs reflect exactly what happens on the spectrometer hardware. You may specify the duration of the simulation in terms of seconds or number of scans. The pulse program output is recorded during this time and visualized on the display. You will find some fine details of a timing sequence, some of immediate delay, within pulse

Top: Shows the tutorial help available with XWIN-NMR™ for 2D processing.

Middle: Explains functionality of the pulse program display software.

Bottom: Explains the fundamentals of writing and using AU programs.

For more information on XWIN-NMR™ software and our other new products, contact your local sales representative.

Chapter 11	10.9 DABY
Chapter 12	10.10 MAZE/NT/AL/MSYS
Chapter 13	10.11 Spectrum Analysis
Chapter 14	11.1 Pulse program simulation (dpp)
Chapter 15	11.2 Parameter (dpp)
Chapter 16	11.3 Page layout (dpp)
Chapter 17	11.4 Page layout for sub-experiments (dpp)
Chapter 18	11.5 Using a prepared page layout (dpp)
Chapter 19	11.6 Defining plot regions
Chapter 20	11.7 Plot Commands
Chapter 21	11.8 Plot status
Chapter 22	11.9 Screen dump
Chapter 23	11.10 Print status parameters
Chapter 24	11.11 Display status parameters
Chapter 25	11.12 Print header labels (dpp)
Chapter 26	11.13 Supported printers
Chapter 27	11.14 The 2D Output Menu
Chapter 28	12.1 Pulse program simulation (dpp)
Chapter 29	12.2 Parameter (dpp)
Chapter 30	12.3 Page layout contour plot (dpp)
Chapter 31	12.4 Page layout stacked plot (dpp)
Chapter 32	12.5 Use prepared page layout (dpp)
Chapter 33	12.6 Defining plot regions
Chapter 34	12.7 Plot Commands
Chapter 35	12.8 Plot status
Chapter 36	12.9 Screen dump
Chapter 37	12.10 Print status parameters
Chapter 38	12.11 Display status parameters
Chapter 39	12.12 Print header labels (dpp)
Chapter 40	12.13 Supported printers
Chapter 41	12.14 The 2D Output Menu
Chapter 42	13.1 Pulse program simulation (dpp)
Chapter 43	13.2 Parameter (dpp)
Chapter 44	13.3 Page layout contour plot (dpp)
Chapter 45	13.4 Page layout stacked plot (dpp)
Chapter 46	13.5 Use prepared page layout (dpp)
Chapter 47	13.6 Defining plot regions
Chapter 48	13.7 Plot Commands
Chapter 49	13.8 Plot status
Chapter 50	13.9 Screen dump
Chapter 51	13.10 Print status parameters
Chapter 52	13.11 Display status parameters
Chapter 53	13.12 Print header labels (dpp)
Chapter 54	13.13 Supported printers
Chapter 55	13.14 The 2D Output Menu
Chapter 56	14.1 Pulse program simulation (dpp)
Chapter 57	14.2 Parameter (dpp)
Chapter 58	14.3 Page layout contour plot (dpp)
Chapter 59	14.4 Page layout stacked plot (dpp)
Chapter 60	14.5 Use prepared page layout (dpp)
Chapter 61	14.6 Defining plot regions
Chapter 62	14.7 Plot Commands
Chapter 63	14.8 Plot status
Chapter 64	14.9 Screen dump
Chapter 65	14.10 Print status parameters
Chapter 66	14.11 Display status parameters
Chapter 67	14.12 Print header labels (dpp)
Chapter 68	14.13 Supported printers
Chapter 69	14.14 The 2D Output Menu
Chapter 70	15.1 Pulse program simulation (dpp)
Chapter 71	15.2 Parameter (dpp)
Chapter 72	15.3 Page layout contour plot (dpp)
Chapter 73	15.4 Page layout stacked plot (dpp)
Chapter 74	15.5 Use prepared page layout (dpp)
Chapter 75	15.6 Defining plot regions
Chapter 76	15.7 Plot Commands
Chapter 77	15.8 Plot status
Chapter 78	15.9 Screen dump
Chapter 79	15.10 Print status parameters
Chapter 80	15.11 Display status parameters
Chapter 81	15.12 Print header labels (dpp)
Chapter 82	15.13 Supported printers
Chapter 83	15.14 The 2D Output Menu
Chapter 84	16.1 Pulse program simulation (dpp)
Chapter 85	16.2 Parameter (dpp)
Chapter 86	16.3 Page layout contour plot (dpp)
Chapter 87	16.4 Page layout stacked plot (dpp)
Chapter 88	16.5 Use prepared page layout (dpp)
Chapter 89	16.6 Defining plot regions
Chapter 90	16.7 Plot Commands
Chapter 91	16.8 Plot status
Chapter 92	16.9 Screen dump
Chapter 93	16.10 Print status parameters
Chapter 94	16.11 Display status parameters
Chapter 95	16.12 Print header labels (dpp)
Chapter 96	16.13 Supported printers
Chapter 97	16.14 The 2D Output Menu
Chapter 98	17.1 Pulse program simulation (dpp)
Chapter 99	17.2 Parameter (dpp)
Chapter 100	17.3 Page layout contour plot (dpp)
Chapter 101	17.4 Page layout stacked plot (dpp)
Chapter 102	17.5 Use prepared page layout (dpp)
Chapter 103	17.6 Defining plot regions
Chapter 104	17.7 Plot Commands
Chapter 105	17.8 Plot status
Chapter 106	17.9 Screen dump
Chapter 107	17.10 Print status parameters
Chapter 108	17.11 Display status parameters
Chapter 109	17.12 Print header labels (dpp)
Chapter 110	17.13 Supported printers
Chapter 111	17.14 The 2D Output Menu
Chapter 112	18.1 Pulse program simulation (dpp)
Chapter 113	18.2 Parameter (dpp)
Chapter 114	18.3 Page layout contour plot (dpp)
Chapter 115	18.4 Page layout stacked plot (dpp)
Chapter 116	18.5 Use prepared page layout (dpp)
Chapter 117	18.6 Defining plot regions
Chapter 118	18.7 Plot Commands
Chapter 119	18.8 Plot status
Chapter 120	18.9 Screen dump
Chapter 121	18.10 Print status parameters
Chapter 122	18.11 Display status parameters
Chapter 123	18.12 Print header labels (dpp)
Chapter 124	18.13 Supported printers
Chapter 125	18.14 The 2D Output Menu
Chapter 126	19.1 Pulse program simulation (dpp)
Chapter 127	19.2 Parameter (dpp)
Chapter 128	19.3 Page layout contour plot (dpp)
Chapter 129	19.4 Page layout stacked plot (dpp)
Chapter 130	19.5 Use prepared page layout (dpp)
Chapter 131	19.6 Defining plot regions
Chapter 132	19.7 Plot Commands
Chapter 133	19.8 Plot status
Chapter 134	19.9 Screen dump
Chapter 135	19.10 Print status parameters
Chapter 136	19.11 Display status parameters
Chapter 137	19.12 Print header labels (dpp)
Chapter 138	19.13 Supported printers
Chapter 139	19.14 The 2D Output Menu
Chapter 140	20.1 Pulse program simulation (dpp)
Chapter 141	20.2 Parameter (dpp)
Chapter 142	20.3 Page layout contour plot (dpp)
Chapter 143	20.4 Page layout stacked plot (dpp)
Chapter 144	20.5 Use prepared page layout (dpp)
Chapter 145	20.6 Defining plot regions
Chapter 146	20.7 Plot Commands
Chapter 147	20.8 Plot status
Chapter 148	20.9 Screen dump
Chapter 149	20.10 Print status parameters
Chapter 150	20.11 Display status parameters
Chapter 151	20.12 Print header labels (dpp)
Chapter 152	20.13 Supported printers
Chapter 153	20.14 The 2D Output Menu
Chapter 154	21.1 Pulse program simulation (dpp)
Chapter 155	21.2 Parameter (dpp)
Chapter 156	21.3 Page layout contour plot (dpp)
Chapter 157	21.4 Page layout stacked plot (dpp)
Chapter 158	21.5 Use prepared page layout (dpp)
Chapter 159	21.6 Defining plot regions
Chapter 160	21.7 Plot Commands
Chapter 161	21.8 Plot status
Chapter 162	21.9 Screen dump
Chapter 163	21.10 Print status parameters
Chapter 164	21.11 Display status parameters
Chapter 165	21.12 Print header labels (dpp)
Chapter 166	21.13 Supported printers
Chapter 167	21.14 The 2D Output Menu
Chapter 168	22.1 Pulse program simulation (dpp)
Chapter 169	22.2 Parameter (dpp)
Chapter 170	22.3 Page layout contour plot (dpp)
Chapter 171	22.4 Page layout stacked plot (dpp)
Chapter 172	22.5 Use prepared page layout (dpp)
Chapter 173	22.6 Defining plot regions
Chapter 174	22.7 Plot Commands
Chapter 175	22.8 Plot status
Chapter 176	22.9 Screen dump
Chapter 177	22.10 Print status parameters
Chapter 178	22.11 Display status parameters
Chapter 179	22.12 Print header labels (dpp)
Chapter 180	22.13 Supported printers
Chapter 181	22.14 The 2D Output Menu
Chapter 182	23.1 Pulse program simulation (dpp)
Chapter 183	23.2 Parameter (dpp)
Chapter 184	23.3 Page layout contour plot (dpp)
Chapter 185	23.4 Page layout stacked plot (dpp)
Chapter 186	23.5 Use prepared page layout (dpp)
Chapter 187	23.6 Defining plot regions
Chapter 188	23.7 Plot Commands
Chapter 189	23.8 Plot status
Chapter 190	23.9 Screen dump
Chapter 191	23.10 Print status parameters
Chapter 192	23.11 Display status parameters
Chapter 193	23.12 Print header labels (dpp)
Chapter 194	23.13 Supported printers
Chapter 195	23.14 The 2D Output Menu
Chapter 196	24.1 Pulse program simulation (dpp)
Chapter 197	24.2 Parameter (dpp)
Chapter 198	24.3 Page layout contour plot (dpp)
Chapter 199	24.4 Page layout stacked plot (dpp)
Chapter 200	24.5 Use prepared page layout (dpp)
Chapter 201	24.6 Defining plot regions
Chapter 202	24.7 Plot Commands
Chapter 203	24.8 Plot status
Chapter 204	24.9 Screen dump
Chapter 205	24.10 Print status parameters
Chapter 206	24.11 Display status parameters
Chapter 207	24.12 Print header labels (dpp)
Chapter 208	24.13 Supported printers
Chapter 209	24.14 The 2D Output Menu
Chapter 210	25.1 Pulse program simulation (dpp)
Chapter 211	25.2 Parameter (dpp)
Chapter 212	25.3 Page layout contour plot (dpp)
Chapter 213	25.4 Page layout stacked plot (dpp)
Chapter 214	25.5 Use prepared page layout (dpp)
Chapter 215	25.6 Defining plot regions
Chapter 216	25.7 Plot Commands
Chapter 217	25.8 Plot status
Chapter 218	25.9 Screen dump
Chapter 219	25.10 Print status parameters
Chapter 220	25.11 Display status parameters
Chapter 221	25.12 Print header labels (dpp)
Chapter 222	25.13 Supported printers
Chapter 223	25.14 The 2D Output Menu
Chapter 224	26.1 Pulse program simulation (dpp)
Chapter 225	26.2 Parameter (dpp)
Chapter 226	26.3 Page layout contour plot (dpp)
Chapter 227	26.4 Page layout stacked plot (dpp)
Chapter 228	26.5 Use prepared page layout (dpp)
Chapter 229	26.6 Defining plot regions
Chapter 230	26.7 Plot Commands
Chapter 231	26.8 Plot status
Chapter 232	26.9 Screen dump
Chapter 233	26.10 Print status parameters
Chapter 234	26.11 Display status parameters
Chapter 235	26.12 Print header labels (dpp)
Chapter 236	26.13 Supported printers
Chapter 237	26.14 The 2D Output Menu
Chapter 238	27.1 Pulse program simulation (dpp)
Chapter 239	27.2 Parameter (dpp)
Chapter 240	27.3 Page layout contour plot (dpp)
Chapter 241	27.4 Page layout stacked plot (dpp)
Chapter 242	27.5 Use prepared page layout (dpp)
Chapter 243	27.6 Defining plot regions
Chapter 244	27.7 Plot Commands
Chapter 245	27.8 Plot status
Chapter 246	27.9 Screen dump
Chapter 247	27.10 Print status parameters
Chapter 248	27.11 Display status parameters
Chapter 249	27.12 Print header labels (dpp)
Chapter 250	27.13 Supported printers
Chapter 251	27.14 The 2D Output Menu
Chapter 252	28.1 Pulse program simulation (dpp)
Chapter 253	28.2 Parameter (dpp)
Chapter 254	28.3 Page layout contour plot (dpp)
Chapter 255	28.4 Page layout stacked plot (dpp)
Chapter 256	28.5 Use prepared page layout (dpp)
Chapter 257	28.6 Defining plot regions
Chapter 258	28.7 Plot Commands
Chapter 259	28.8 Plot status
Chapter 260	28.9 Screen dump
Chapter 261	28.10 Print status parameters
Chapter 262	28.11 Display status parameters
Chapter 263	28.12 Print header labels (dpp)
Chapter 264	28.13 Supported printers
Chapter 265	28.14 The 2D Output Menu
Chapter 266	29.1 Pulse program simulation (dpp)
Chapter 267	29.2 Parameter (dpp)
Chapter 268	29.3 Page layout contour plot (dpp)
Chapter 269	29.4 Page layout stacked plot (dpp)
Chapter 270	29.5 Use prepared page layout (dpp)
Chapter 271	29.6 Defining plot regions
Chapter 272	29.7 Plot Commands
Chapter 273	29.8 Plot status
Chapter 274	29.9 Screen dump
Chapter 275	29.10 Print status parameters
Chapter 276	29.11 Display status parameters
Chapter 277	29.12 Print header labels (dpp)
Chapter 278	29.13 Supported printers
Chapter 279	29.14 The 2D Output Menu
Chapter 280	30.1 Pulse program simulation (dpp)
Chapter 281	30.2 Parameter (dpp)
Chapter 282	30.3 Page layout contour plot (dpp)
Chapter 283	30.4 Page layout stacked plot (dpp)
Chapter 284	30.5 Use prepared page layout (dpp)
Chapter 285	30.6 Defining plot regions
Chapter 286	30.7 Plot Commands
Chapter 287	30.8 Plot status
Chapter 288	30.9 Screen dump
Chapter 289	30.10 Print status parameters
Chapter 290	30.11 Display status parameters
Chapter 291	30.12 Print header labels (dpp)
Chapter 292	30.13 Supported printers
Chapter 293	30.14 The 2D Output Menu
Chapter 294	31.1 Pulse program simulation (dpp)
Chapter 295	31.2 Parameter (dpp)
Chapter 296	31.3 Page layout contour plot (dpp)
Chapter 297	31.4 Page layout stacked plot (dpp)
Chapter 298	31.5 Use prepared page layout (dpp)
Chapter 299	31.6 Defining plot regions
Chapter 300	31.7 Plot Commands
Chapter 301	31.8 Plot status
Chapter 302	31.9 Screen dump
Chapter 303	31.10 Print status parameters
Chapter 304	31.11 Display status parameters
Chapter 305	31.12 Print header labels (dpp)
Chapter 306	31.13 Supported printers
Chapter 307	31.14 The 2D Output Menu
Chapter 308	32.1 Pulse program simulation (dpp)
Chapter 309	32.2 Parameter (dpp)
Chapter 310	32.3 Page layout contour plot (dpp)
Chapter 311	32.4 Page layout stacked plot (dpp)
Chapter 312	32.5 Use prepared page layout (dpp)
Chapter 313	32.6 Defining plot regions
Chapter 314	32.7 Plot Commands
Chapter 315	32.8 Plot status
Chapter 316	32.9 Screen dump
Chapter 317	32.10 Print status parameters
Chapter 318	32.11 Display status parameters
Chapter 319	32.12 Print header labels (dpp)
Chapter 320	32.13 Supported printers
Chapter 321	32.14 The 2D Output Menu
Chapter 322	33.1 Pulse program simulation (dpp)
Chapter 323	33.2 Parameter (dpp)
Chapter 324	33.3 Page layout contour plot (dpp)
Chapter 325	33.4 Page layout stacked plot (dpp)
Chapter 326	33.5 Use prepared page layout (dpp)
Chapter 327	33.6 Defining plot regions
Chapter 328	33.7 Plot Commands
Chapter 329	33.8 Plot status

## Sandia National Laboratories

Albuquerque, New Mexico 87185-1407

LOCKHEED MARTIN

Dr. B. L. Shapiro  
The NMR Newsletter  
966 Elsinore Court  
Palo Alto, CA 94303

25 October, 1995  
(received 10/30/95)

### Revisiting the INEPT Pulse Sequence and $^{29}\text{Si}$ NMR Identification of Initial Condensation Products in Organoalkoxysilanes<sup>1</sup>

Dear Barry,

A continuing research area at Sandia National Labs is the development and characterization of new materials produced from organically modified alkoxy silanes. Using  $^{29}\text{Si}$  NMR the kinetics of polymerization in these sol-gel materials can be investigated. In recent studies of methyltrimethoxysilane (MTMS) sol-gel systems the assignment of  $^{29}\text{Si}$  NMR resonances for the hydrolysis and initial condensation products were complicated by an unusual small spectral dispersion ( $\sim 0.5$  ppm). This is in contrast to previous studies of tetraalkoxysilane systems where  $^{29}\text{Si}$  resonances assignments are typically based on a substantial downfield shift with increasing hydroxyl number. To aid in assignments for the MTMS systems, the INEPT sequence has been utilized to distinguish various silicon environments, correcting assignments based solely on chemical shift arguments. The INEPT sequence not only proves useful for spectral editing but affords polarization transfer to silicon, a nucleus plagued by long relaxation times and a negative NOE. For MTMS and the resulting hydrolysis and condensation products there are between 12 and 3 protons coupled to each silicon. In addition, there are two different heteronuclear couplings,  $J(\text{Si},\text{H}) = 8.3$  Hz and  $J(\text{Si},\text{H}) = 3.9$  Hz for the methyl and methoxy groups respectively, giving rise to a complicated response for the polarization

transfer. The protons for attached hydroxyl groups are in rapid exchange and reveal no coupling to the silicon, allowing the degree of hydrolysis to be investigated using the INEPT sequence. For example, the response of these  $\text{IS}_3\text{S}_m$  ( $m = 0, 3, 6$ ) spin systems (as expected in the condensation products) during an INEPT experiment as a function of the refocusing delay  $\Delta$  is shown in Fig. 1. For MTMS the silicon types are denoted as  $\text{T}_m^n$  where  $m$  represents the number of hydroxyl groups and  $n$  the number of siloxane bonds in the unit of  $\text{CH}_3\text{Si}(\text{O}_{0.5})_n(\text{OH})_m(\text{OCH}_3)_{3-m-n}$ .

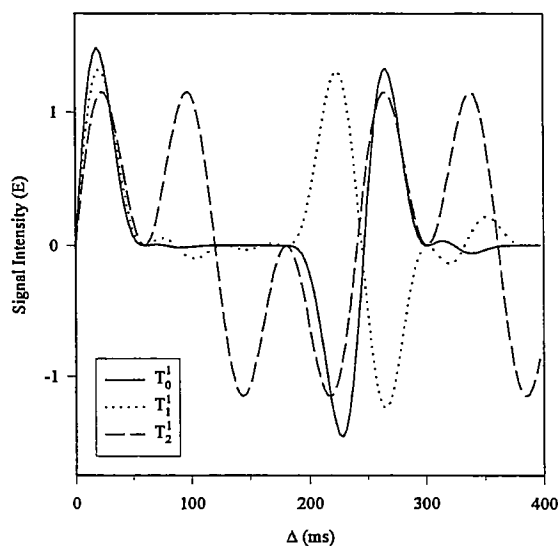


**Figure 1.** Theoretical signal intensity for the initial condensation products of MTMS following the INEPT pulse sequence as a function of the refocusing time  $\Delta$ , for  $J(\text{Si},\text{H}) = 8.3$  Hz and  $J(\text{Si},\text{H}) = 3.9$  Hz. The lines (—),  $\text{T}_0^1$ , (.....)  $\text{T}_1^1$  and (---)  $\text{T}_2^1$  correspond to  $\text{IS}_3\text{S}_6$ ,  $\text{IS}_3\text{S}_3$ ,  $\text{IS}_3\text{S}_0$  spin systems, respectively.

<sup>1</sup> This work is supported by the US Department of Energy under Contract DE-AC04-94AL85000.

For the initial condensation products of MTMS there are three different silicon types present,  $T_0^I$ ,  $T_1^I$  and  $T_2^I$ . With nearest neighbor effects 9 distinct resonances are expected for the  $T^I$ - $T^I$  condensation products. Inspection of Fig. 1 reveal the  $T_1^I$  silicon species is easily distinguished from the  $T_0^I$  and  $T_2^I$  species using the INEPT experiment with a refocusing delay of  $\Delta = 220$  ms. The  $T_2^I$  resonance can be distinguished by noting that this is the only signal at  $\Delta = 90$  and 150 ms. By combining these experiments identification of the various silicon types becomes possible. As an example consider the  $T^I$  condensation products for a 2.24 M solution of MTMS in MeOH, with a 1.5 molar equivalent of  $H_2O$  ( $R=1.5$ ) as shown in Fig. 2. These INEPT experiments were performed at 9.4 Tesla using a 5 mm broadband probe. Only the signals G,H,I are present at  $\Delta = 90$  and 150 ms (not shown) allowing the assignment of these as  $T_2^I$  resonances. Experiments performed at  $\Delta = 20$  and 220 ms easily allows the assignment of  $T_1^I$  species (Fig. 2). Using these results, plus the correlation of signal intensities into pairs, all of the condensation products are easily identified. It is interesting to note the chiral  $T_1^I$  silicons give rise to two distinct resonances in the condensed species  $T_1^I - T_1^I$ , denoted as resonances D and D'. These initial results are very encouraging, and provide an additional tool for the investigation of silicon containing systems.

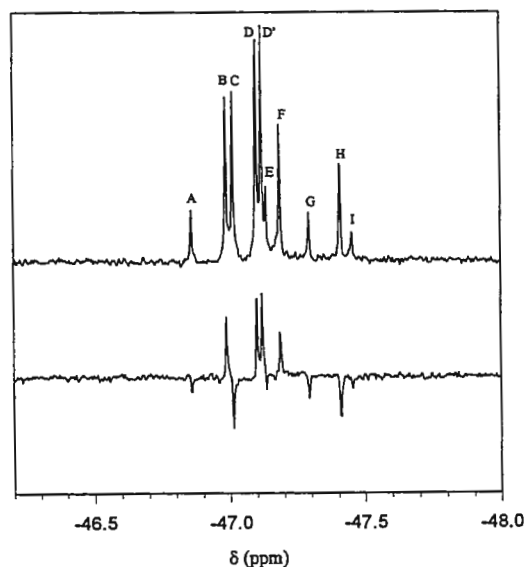


**Figure 2.**  $^{29}\text{Si}$  NMR INEPT spectra of the  $T^I$  condensation products after 60 minutes for a 2.24 M MTMS/MeOH solution with  $R=1.5$   $H_2O$  added. Spectra are for refocusing delays of  $\Delta = 20$  ms (top) and 220 ms (bottom). The resonances can be assigned to;

$A = \underline{T_0^I} - \underline{T_0^I}$ ,  $B = \underline{T_1^I} - \underline{T_0^I}$ ,  $C = \underline{T_1^I} - \underline{T_0^I}$ ,  $D$  and  $D' = \underline{T_1^I} - \underline{T_1^I}$ ,  $E = \underline{T_0^I} - \underline{T_2^I}$ ,  $F = \underline{T_1^I} - \underline{T_2^I}$ ,  $G = \underline{T_0^I} - \underline{T_2^I}$ ,  $H = \underline{T_1^I} - \underline{T_2^I}$ , and  $I = \underline{T_2^I} - \underline{T_2^I}$ , where the underscore designates the silicon of interest.

Cheers,

*Todd Alam*

Todd Alam

*Roger Assink*

Roger Assink





UNIVERSITY OF MISSOURI-ROLLA  
Missouri's Technological University

Frank D. Blum  
Department of Chemistry  
142 Schrenk Hall  
Rolla, Missouri 65401-0249  
(314)-341-4451 (or 4420)  
fblum@umr.edu

Dr. Bernard L. Shapiro  
966 Elsinore Court  
Palo Alto, CA 94303

November 18, 1995  
(received 11/24/95)

### Molecular Dynamics of Sodium n-Alkylbenzenesulfonate Adsorbed onto Alumina

Dear Barry:

We have been utilizing deuterium NMR to investigate the molecular dynamics of surfactants adsorbed onto alumina particles in aqueous solution. A prototype surfactant, isomerically pure sodium n-decylbenzenesulfonate-d<sub>4</sub>, was synthesized in our laboratory, and g-alumina (D=10 nm, BET specific surface area=79 m<sup>2</sup>/g) was purchased from Johnson Matthey Electronics Co. Ltd. Four surfactant-adsorbed alumina samples with different coverages were prepared at pH 4, 40 °C and transferred to 1.9 mm  $\phi$  8 mm glass tubes after sedimentation. A Doty wide-line probe was used with the quadrupolar echo sequence at 61.395 MHz (400 MHz) on a Varian VXR/S-200/400. All the spectra were referenced to D<sub>2</sub>O-H<sub>2</sub>O (1:1 volume)

The adsorption isotherm of the surfactant onto oppositely charged alumina particles is shown in the log equilibrium concentration — log adsorption amount plots. The four discrete regions labelled as Region 1, 2, 3, and 4 are typical characteristics of ionic surfactant adsorption onto mineral oxides, which represents different adsorption states of surfactant molecules on the surfaces.

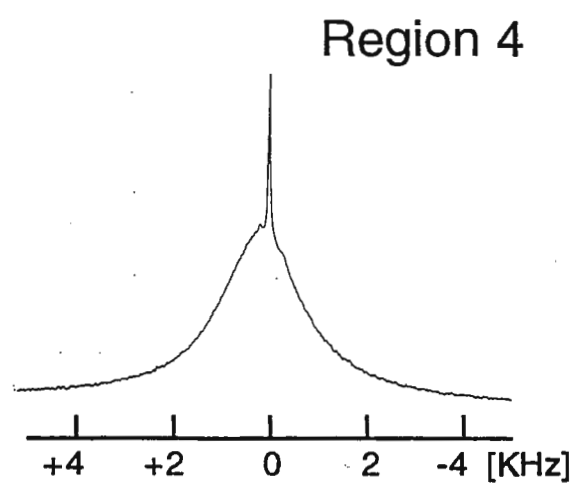
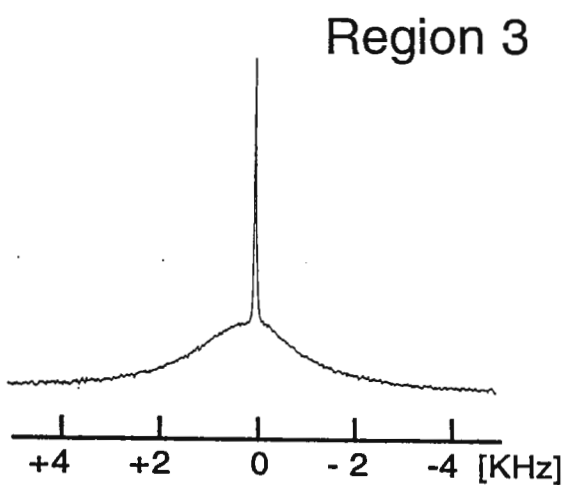
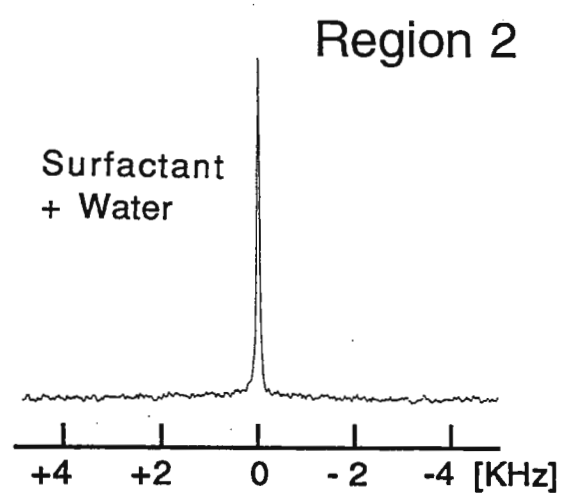
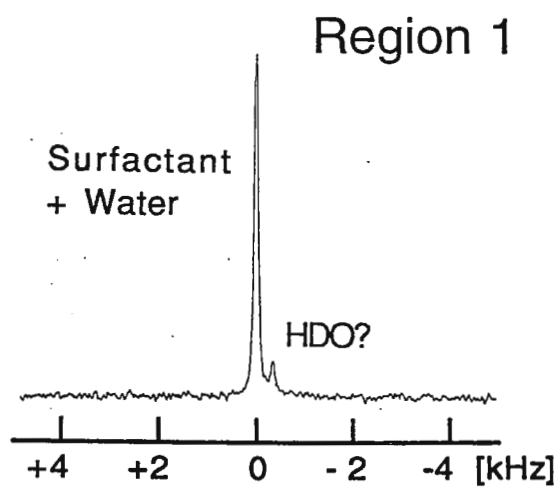
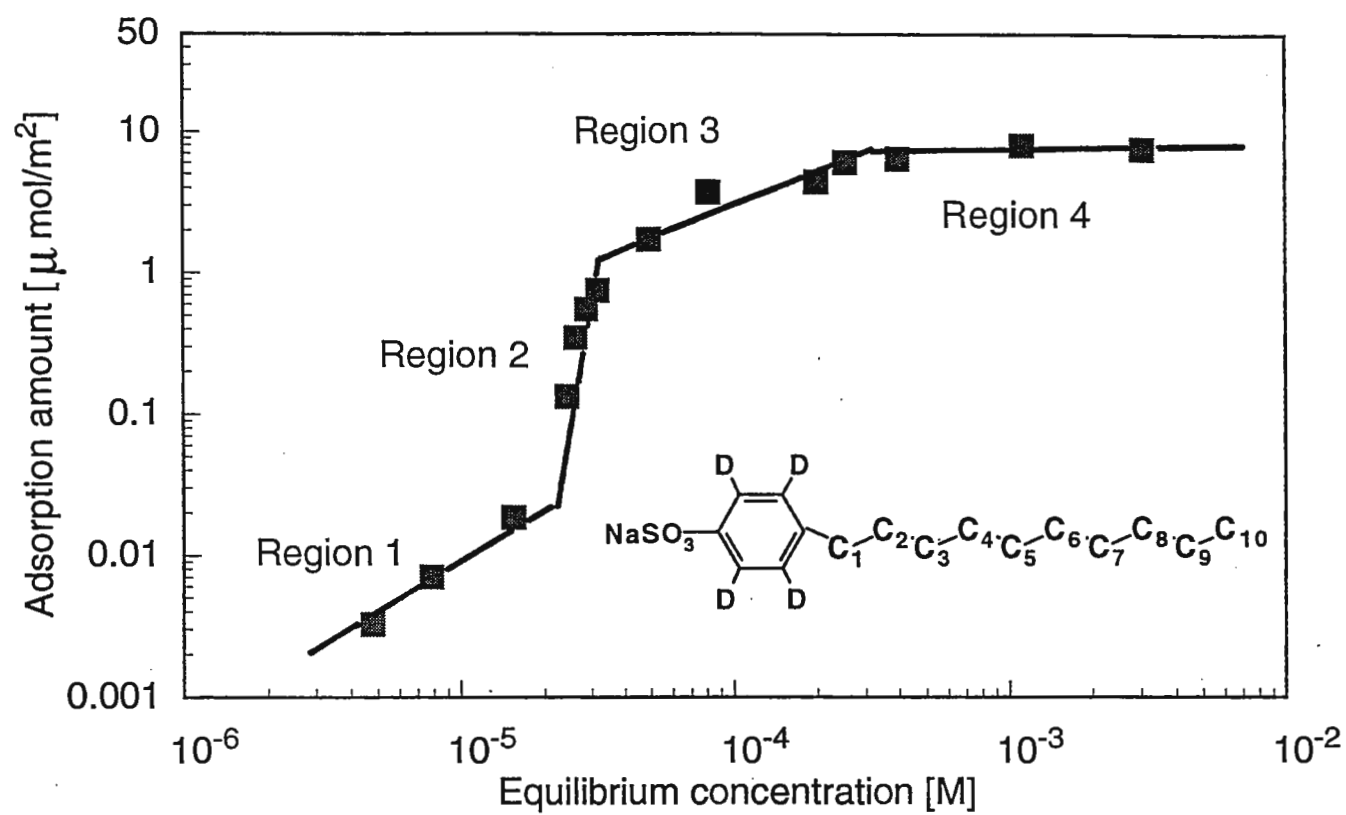
Based on the isotherm, deuterium NMR spectra in each region were obtained to elucidate the adsorption mechanisms. Region 1 and 2 gave relatively narrow single resonances reflecting the rapid molecular motion of the surfactant on the pertinent NMR time scale. This is attributable to fast exchange between the surfactant molecules on the surface and the monomers in the solution phase. Another possible reason for this is that the molecules may diffuse around a particle during one pulse sequence since the lateral diffusion of surfactant molecules on the surface may be quite fast. (The small resonance on Region 1 (-0.36 kHz) is tentatively identified to be that from a small number of water molecules in pores on the alumina surface or interstices between the agglomerates) In these dilute regimes, the surfactants probably form monolayers in which the surfactant molecules are rapidly reorienting with the polar groups more or less close to the alumina surface. Quantitative analysis confirms that the narrow resonances is significantly broadened at the end of Region 2, and regains the original intensity at the onset of Region 4. The Region 3 spectrum acquires another noticeably broad resonance overlapping the narrow resonances from the surfactant and HDO. This phenomenon implies the possible formation of an outer layer (i.e. bilayer formation) where the alkyl chains orient inwards and the polar groups outwards. In Region 4 where saturation adsorption is established, further growth of broadened portion is observable correlating with an increase in total amount adsorbed.

Best regards,

K. Nagashima

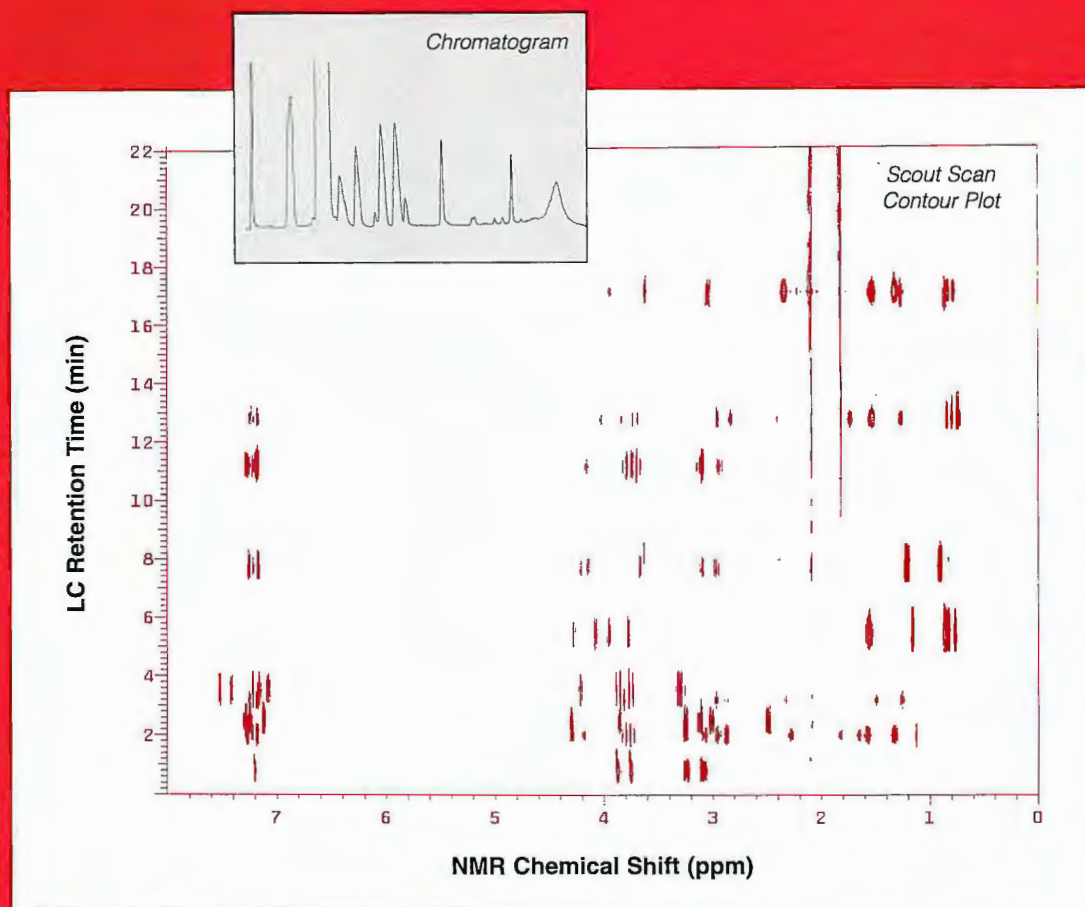
Kazuomi NAGASHIMA  
e-mail : nagashma@ibm530.chem.umn.edu

Frank D. Blum  
Curators' Professor of Chemistry  
fblum@umr.edu





# LC-NMR: Separations and Structures



*On-flow 500 MHz  $^1\text{H}$  LC-NMR data of a peptide mixture using Scout Scan and WET solvent suppression during an LC gradient. The sample was a 100  $\mu\text{L}$  injection of  $\sim 1\text{ mg/mL}$  peptides separated using a  $\text{CH}_3\text{CN}:\text{D}_2\text{O}$  solvent gradient (5%  $\text{CH}_3\text{CN}$  to 50% in 22 min).*

Combining the superior separation capabilities of HPLC with the exceptional structure elucidation capabilities of NMR, Varian's exciting new LC-NMR accessory is the most powerful and versatile tool for examining the chemical structures of complex mixtures.

Recent advances in the areas of NMR sensitivity, multiple solvent suppression, modular design, and the control of hardware on-the-fly have made the use of LC-NMR truly practical for solving difficult research problems. As drug and other product development cycles decrease, laboratories worldwide are taking advantage of new technologies

which directly impact time-to-market. This innovative hyphenated technique eliminates the need for time-consuming sample isolation and purification steps, thereby streamlining research efforts and liberating resources.

Available for all UNITY NMR spectrometers including the new <sup>UNITY</sup>INOVA, the LC-NMR accessory includes a flow NMR probe, a complete LC system (pump, variable wavelength UV detector, PC, column, etc.), a peak sense module, an interface between the LC and NMR systems, and a comprehensive LC-NMR software package.

**varian** 

## Features

## Benefits

- Multiple NMR flow cell volumes.....Optimizes chromatographic resolution and S/N for flow and fraction collection methods
- Peak sense module.....Automatically positions analyte in NMR probe coil region based on UV or other HPLC detector signal
- Multiple HPLC detectors.....Variety of detectors ensures that most chemical species can trigger stop-flow NMR acquisitions
- Modularity of analyte collector.....True off-line fraction collection capability provides optimal utilization of NMR spectrometer
- Flexibility of analyte collector.....Generic loop collector module provides compatibility with other LC equipment
- Scout Scan™.....Perfectly adjusted, on-the-fly solvent suppression for on-flow and stop-flow LC gradient applications
- WET solvent suppression.....Combination of selective excitation with pulsed field gradients optimizes multiple peak solvent suppression
- <sup>13</sup>C sideband suppression.....Efficient removal of <sup>13</sup>C sidebands of non-deuterated solvent peaks provides a cleaner NMR spectrum for analyte identification
- NMR "time slicing" of chromatogram.....Facilitates identification of individual components from unresolved or coeluting species
- Compatible with non-deuterated organic solvents.....Excellent solvent suppression removes the requirement for costly deuterated solvents such as CD<sub>3</sub>CN and CD<sub>3</sub>OH
- Compatible with non-volatile buffers.....Easily allows study of buffered systems which are very difficult for LC-MS
- Powerful & flexible VNMR software.....Variety of processing and display macros allows facile examination of LC-NMR data
- Control of LC injections from NMR console.....Advanced interface allows operator to initiate LC-NMR experiment from NMR console
- Hypertext, linked on-line LC-NMR manual.....Dramatically reduces the learning curve for LC-NMR operation at the spectrometer

## LC-NMR Applications

- Drug metabolism
- Drug impurity assays
- Coeluting compounds
- Fermentation studies
- Clinical chemistry
- Peptide synthesis
- Purity of bulk materials
- Synthetic chemistry monitoring
- Lability and degradation studies
- Isomeric ratios for synthetic reactions
- Extent of polymerization
- Functionalization of synthetic polymers
- Chemical waste analysis
- Reaction kinetics
- Molecular complexation
- Monitoring of chemical reactions on-line
- Quality control
- Transition state monitoring
- Tautomerism monitoring

**Manufacturing Facilities** Varian NMR Instruments, Building 4, 3120 Hansen Way, Palo Alto, California 94304-1030, Tel 415.493.4000

• **Australia** Mulgrave, Victoria, Tel 3.9.560.7133 • **Austria** Vösendorf, Tel 1.69.5445 • **Belgium** Brussels, Tel 2.721.4850 • **Brazil** São Paulo, Tel 11.820.0444  
 • **Canada** Mississauga, Ontario, Tel 1.800.387.2216 • **China** Beijing, Tel 1.256.4360 • **France** Les Ulis, Tel 1.6986.3838 • **Germany** Darmstadt, Tel 06151.7030  
 • **Italy** Milan, Tel 2.921351 • **Japan** Tokyo, Tel 3.5232.1211 • **Korea** Songtan City, Tel 333.665.5171 • **Mexico** Mexico City, Tel 5.514.9882 • **Netherlands** Houten, Tel 3403.50909 • **Russian Federation** Moscow, Tel 095.203.7925 • **Spain** Madrid, Tel 91.472.7612 • **Sweden** Solna, Tel 8.82.00.30 • **Switzerland** Zug, Tel 42.448.844 • **Taiwan** Taipei, Tel 2.705.3300 • **United Kingdom** Walton-on-Thames, Tel 01932.898.000 • **United States** California, Tel 800.356.4437  
 • Other sales offices and dealers throughout the world

**varian** 



## UNIVERSITY OF CALIFORNIA, BERKELEY

BERKELEY DAVIS IRVINE LOS ANGELES RIVERSIDE SAN DIEGO SAN FRANCISCO



SANTA BARBARA SANTA CRUZ

Jeffrey A. Reimer

Professor

reimer@garnet.berkeley.edu

 Department of Chemical Engineering  
 Berkeley, California 94720-1462  
 (510) 642-8011 FAX: (510) 642-4778

NMR with electronically conductive samples

Dear Barry:

November 16, 1995

(received 11/21/95)

One exciting area of research currently being pursued in our lab is the study of adsorbates on electrocatalyst surfaces. A necessary constraint in electrochemical systems is a sufficiently high electrical conductivity to prevent ohmic losses. It has been shown that such a constraint results in coupling of the sample to the coil of an NMR probe<sup>1-3</sup>. Since it is our desire to perform *in-situ* experiments, we have been forced to develop a better understanding of the physical interactions of a solenoid and an electronically conducting sample.

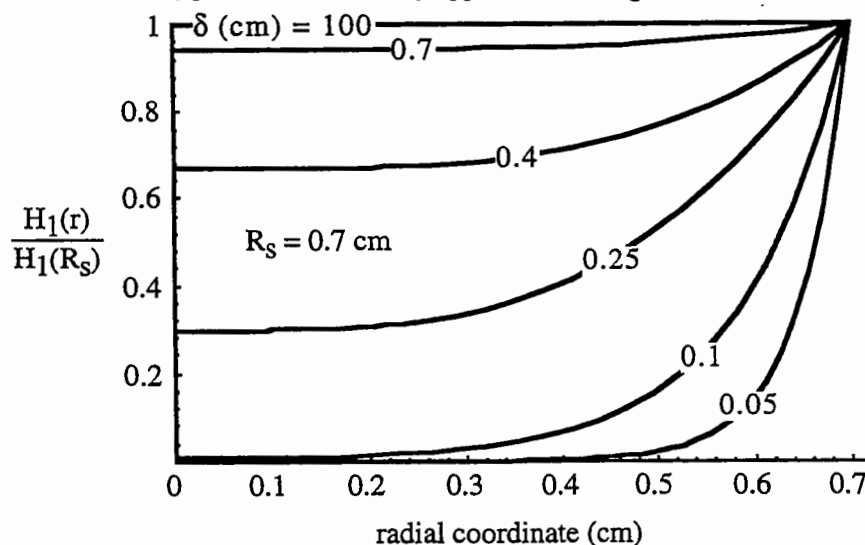
In an ideal NMR experiment the *rf* field will be constant everywhere in the sample. As conduction electrons become mobile, however, a loss mechanism is provided via Ohm's law; the applied field is then expected to vary spatially within the sample. An analytical expression for the field distribution can be derived for the case of a 1-D cylinder using Maxwell's equations. Combining Faraday's and Ampere's laws in MKSA units, and separating spatial and time variables, results in a general second-order differential equation for the *rf* field  $H_1$ :

$$\nabla^2 H_1 = (i\omega\mu\sigma - \mu\epsilon\omega^2)H_1, \quad (1)$$

where  $\sigma$  is the conductivity,  $\mu$  and  $\epsilon$  are the sample permeability and permittivity, respectively. For a sample of appreciable conductivity we can neglect the displacement currents described by the real term on the right side of equation (1), leaving a special form of Bessel's equation. We apply boundary conditions that  $H_1(0)$  is finite and  $H_1(R_s)$  is simply equal to the field in an equivalent coil in the absence of the conductor. The solution for the applied  $H_1$  field in the sample is given by

$$\frac{H_1(r)}{H_1(R_s)} = \frac{J_0\left(\frac{\sqrt{2}}{\delta} r e^{-i\frac{\pi}{4}}\right)}{J_0\left(\frac{\sqrt{2}}{\delta} R_s e^{-i\frac{\pi}{4}}\right)} \quad (2)$$

where  $J_0$  is a Bessel function of order zero, and  $\delta = \left(\frac{2}{\omega\mu\sigma}\right)^{\frac{1}{2}}$  is a characteristic length termed the skin depth. The effect of sample conductivity on *rf* penetration is readily apparent in the figure shown below.



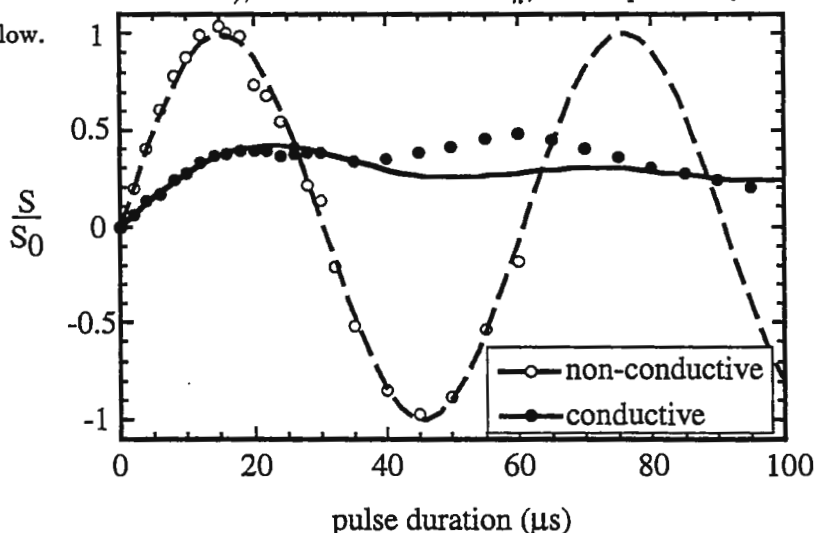
One would expect this distribution of applied fields to affect the nutation behavior of a group of spins distributed throughout a conducting matrix. In order to confirm this we compared results of nutation experiments with conductive and non-conductive samples. Measurements were performed on two samples in our home built 270 MHz spectrometer equipped with a  $^{13}\text{C}$  probe designed to minimize coupling of the sample to the coil. A conductive sample was prepared by soaking  $1\text{-}^{13}\text{C}$ -enriched acetic acid into a 14mm diameter porous graphite plug of known conductivity. The other sample consisted of only  $^{13}\text{C}$ -enriched methanol. Transmitter power was set for  $15\mu\text{s}$   $\frac{\pi}{2}$ -pulses for the methanol sample and amplitudes of the resulting Lorentzian lines from both samples were recorded as a function of pulse length.

In order to fit the data, we recognize that the contribution from an individual nuclear spin in the sample following application of an  $rf$  pulse of magnitude  $H_1$  is related to the magnitude of the component of its magnetic moment in the  $x$ - $y$  plane (with the static  $B_0$  field aligned along the  $z$  axis). A summation over the entire sample yields an expression for the detected signal,  $S$ :

$$\frac{S}{S_0} = \frac{\int_0^{R_s} \sin(\gamma H_1(r) t_p) dV}{\int_0^{R_s} dV} = \frac{2}{R_s^2} \int_0^{R_s} r \sin\left(\omega_n^* t_p \frac{H_1(r)}{H_1(R_s)}\right) dr \quad (3)$$

where  $\omega_n^* = \gamma H_1(R_s) = \frac{2\pi}{t_p(\frac{\pi}{2})}$  and  $\frac{H_1(r)}{H_1(R_s)}$  is given by (2). Numerical techniques were used to fit the data using  $\delta = 0.09\text{cm}$  (based on a measured value of  $\sigma$ ), calculated values for  $\omega_n^*$ , and amplitude  $S_0$  as an adjustable parameter.

The result is shown below.



This simple calculation shows quantitatively how the electrical conductivity of an NMR sample couples inductively to the coil, resulting in attenuation of the applied  $rf$  as the field penetrates the conductor. This spatial variation of the field can cause severe distortion of the nutation function, rendering precise manipulation of sample magnetization difficult, or perhaps impossible. For applications requiring high conductivity, the situation can be improved by investigating methods of sample preparation that minimize the length scales over which eddy currents can propagate<sup>4</sup>.

Jeffrey A. Reimer

Best regards to all,

Mark S. Yahnke

p.s. Please contribute this to the Raychem account.

1. Bloembergen, N. *J. Appl. Phys.* **23** (1952) 1383.
2. Hoult, D. I. and P. C. Lauterbur. *J. Mag. Res.* **34** (1979) 425.
3. Gadian, D. G. and F. N. H. Robinson. *J. Mag. Res.* **34** (1979) 449.
4. Kugel, H. *J. Mag. Res.* **91** (1991) 179.



# Model 3445/3446 Amplifiers from AMT

**10-130 MHz  
Bandwidth**

**1000 and 2000  
watt Models  
available**



## For High Performance NMR/NMRI Applications

Your NMR/NMRI requirements are pushing the leading edge of science and you need AMT RF power technology! The 3446 and 3445 operate from 10-130 MHz and are rated at 1000 watts for low field NMR and up to 2000 watts for NMRI applications up to 3 Tesla. AMT has brought together the highest possible RF performance at a most cost effective price. Nobody builds a better NMR/NMRI amplifier than AMT...

### Additional Features Include:

- 10-130 MHz bandwidth for use in systems up to 3T
- Up to 2000 watts of power for imaging
- CW power capability for decoupling
- Blanking delay time >1  $\mu$ s for multi-pulse



## Models 3445/3446

10-130 MHz, pulsed, solid-state,  
RF power amplifier systems

### Key Specifications:

Models:	3445	3446
Frequency range	10-130 MHz	10-130 MHz
Pulse power (min.) into 50 ohms	2000 W	1000 W
CW power (max.) into 50 ohms	200 W	100 W
Linearity ( $\pm 1$ dB to 30 dB down from rated power)	1500 W	800 W
Pulse width	20 ms	20 ms
Duty cycle	Up to 10%	Up to 10%
Amplitude droop	5% to 20 ms typ.	5% to 20 ms typ.
Harmonics	Second: -25 dBc max. Third: -24 dBc max.	
Phase change/output power	10° to rated power, typ.	
Phase error overpulse	4° to 20 ms duration, typ.	
Output noise (blanked)	< 10 dB over thermal	
Blanking delay	< 1 $\mu$ s on/off, TTL signal	
Blanking duty cycle	Up to 100%	
Protection	1. Infinite VSWR at rated power 2. Input overdrive 3. Over duty cycle/pulse width 4. Over temperature	

### Other members of AMT's NMR/NMRI Family:

#### 3205/3200

6-220 MHz, 300/1000 W

#### 3304/3303

30-310 MHz, 400/700 W

#### PowerMaxx™ series

25-175 MHz, 4kW/7 kW

#### 3137/3135/3134

200-500 MHz, 50/150/300 W

### Supplemental Characteristics:

Indicators, front panel	1. AC power on 2. CW mode	4. Overdrive 5. Over pulse width	6. Over duty cycle 7. LCD peak power meter
System monitors	1. Forward/Reflected RF power 2. Over pulse width/duty cycle	3. DC power supply fault	4. Thermal fault
Front panel controls	1. AC power	2. Forward/Reflected power	
AC line voltage	208/230 VAC, 10%, 1Ø, 47-63 Hz		

	3445	3446
AC power requirements	1400 VA	700 VA
Size (HWL, inches)	8.75 x 19 x 24	8.75 x 19 x 24
Net weight	110 lbs.	75 lbs.



### FOR ADDITIONAL INFORMATION, PLEASE CALL:

AMT United States	Gigatron Associates Canada	Dressler Germany, Switzerland	JEOL Trading Co. Japan	Goss Scientific Instruments United Kingdom, France, Benelux
Ph: (714) 993-0802 Fx: (714) 993-1619	Ph: (613) 225-4090 Fx: (613) 225-4592	Ph: 49 2402 71091 Fx: 49 2402 71095	Ph: 81 3 3342 1921 Fx: 81 3 3342 1944	Ph: 44 1245 478441 Fx: 44 1245 473272

University of Illinois  
at Urbana-Champaign

School of Chemical Sciences  
142B RAL, Box 34-1  
600 S. Mathews Avenue  
Urbana, IL 61801

Telephone: (217) 244-0564  
FAX: (217) 244-8068  
mainzv@aries.scs.uiuc.edu

November 17, 1995 (received 11/20/95)

Dr. B. L. Shapiro  
The NMR Newsletter  
966 Elsinore Court  
Palo Alto, CA 94303

### Decoupler Problem or New Decoupler Test?

Dear Barry:

As Heinz Sterk pointed out in the November newsletter, "Sometimes ... things turn out to be much more complicated than expected at the first glance.". We would like to report some of the problems and solutions encountered recently while setting up a simple experiment.

The simple experiment is a cross-relaxation or magnetization transfer experiment. (J.Y. Wu & T.M. Eads; *Carbohydrate Polymers* **20** (1993) 51-60 and J.Y. Wu; R.G. Bryant & T.M. Eads; *J. Agric. Food Chem.* **40** (1992) 449-455) for detection of solid-like components in gelatinized starch. The experiment is simply a series of presaturation experiments with the presaturation offset frequency varied between -50kHz and +50kHz. The amplitude of the liquid spectra are recorded to give the cross-relaxation spectrum. The cross-relaxation spectrum contains information about the solid component, specifically mobility information.

We expected the experiment to be somewhat demanding of our equipment (GN300s) due to the use of fairly high power presaturation pulses of 4-5 seconds. The presaturation pulses to give proton precession frequencies of 300-500Hz are greater than 1 watt of rf power. Possibly a problem for the standard probe and certain components. Larger resistors were installed in the rf module and care was taken to be sure to have adequate air flow through the probe body.

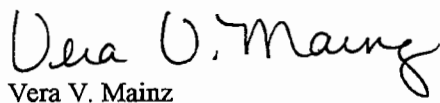
As a test of the experimental setup we looked at the cross-relaxation spectra of water. We had obvious problems when the spectra showed decreased intensities at offset frequencies greater than  $\pm 40$ kHz with a severe dip from +27.5kHz to +37.5kHz. Expected behavior was observed near zero offset; with near zero intensity for offsets within  $\pm 500$ Hz of resonance and constant intensity for offset frequencies between +40kHz and +5kHz and between -5kHz and -20kHz. (see figure) We first questioned whether this was a probe or console problem. Rerunning the experiment with a Chemagnetics MAS probe in place of the liquids probe ruled out a probe related problem due to the fairly high power. Spectra were the same for the two probes.

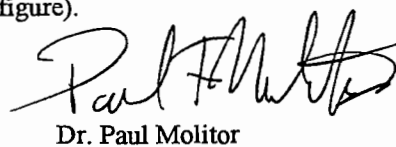
A decrease in power would have been the obvious malfunction. However, the scope trace of the decoupler pulse showed constant rf voltage at all frequencies. Also, a drop in power of the saturation pulse would not be consistent with the spectral evidence. The problem became apparent on closer inspection of the decoupler rf output. As the offset frequency increased the signal became noisy. The transmitter noise having a significant component at the water resonance frequency. This noise component partially saturated the water resonance.

Like many problems the solution was more difficult than characterization. After swapping nearly every logic chip in the rf generation unit we were exactly where we started. We noticed that the scope trace improved with tapping on the chips (last resort type troubleshooting). This led to the speculation that the high-speed chips were not working properly due to poor electrical contact with the sockets. The signal quality improved as each chip was removed and the terminals cleaned. Eventually the unit produced a clean signal at all frequencies.

This was verified by running the cross-relaxation spectrum for water (see figure). Having a correct water spectrum we acquired the now reasonable cross-relaxation spectrum of a starch gel (see figure).

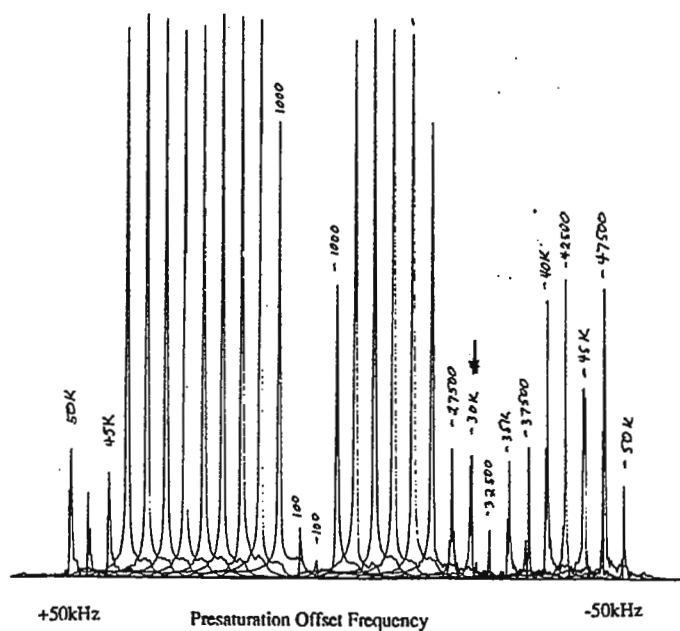
Sincerely,

  
Vera V. Mainz

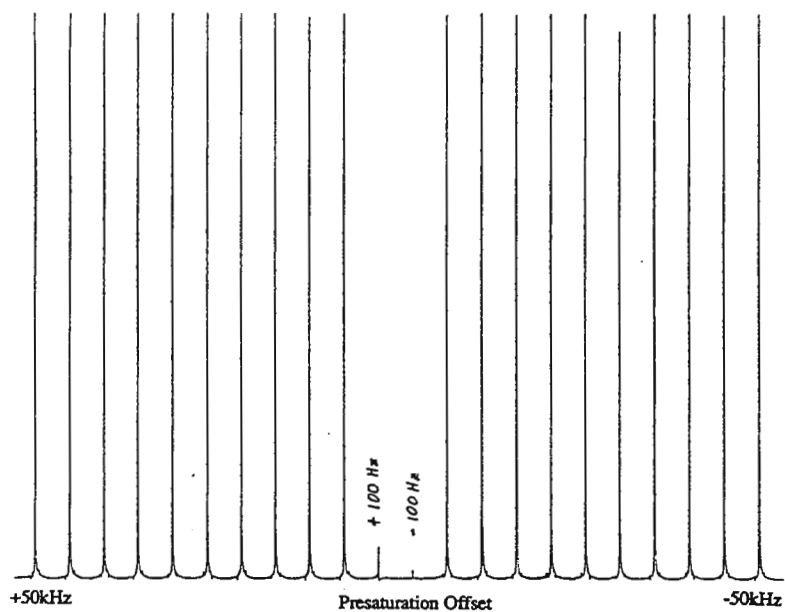
  
Dr. Paul Molitor

Molecular Spectroscopy Laboratory

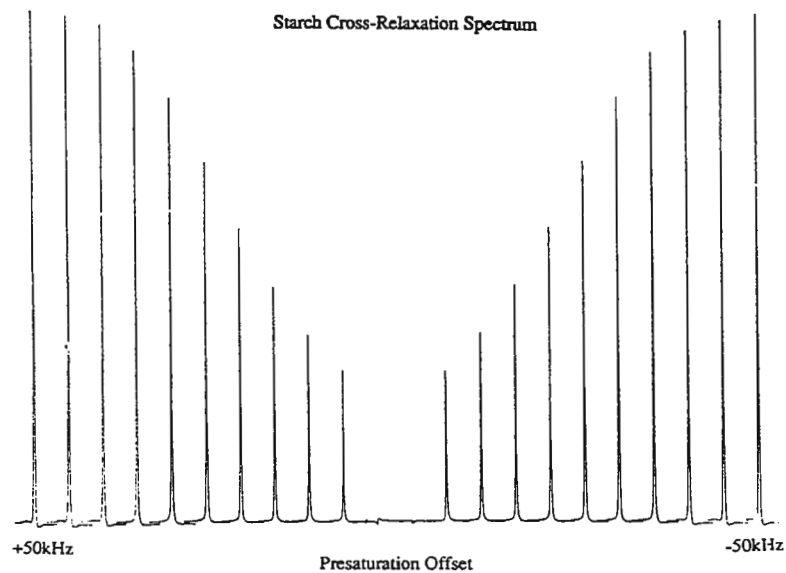




### H<sub>2</sub>O Cross-Relaxation Spectrum



### Starch Cross-Relaxation Spectrum



Flexibility

**Chemagnetics**  
*Innovators in Spectroscopy*

Performance

FEATURES

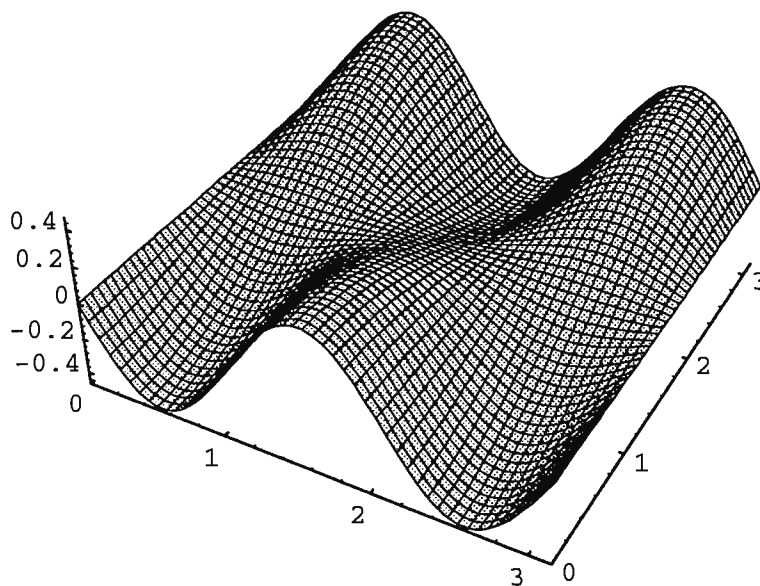
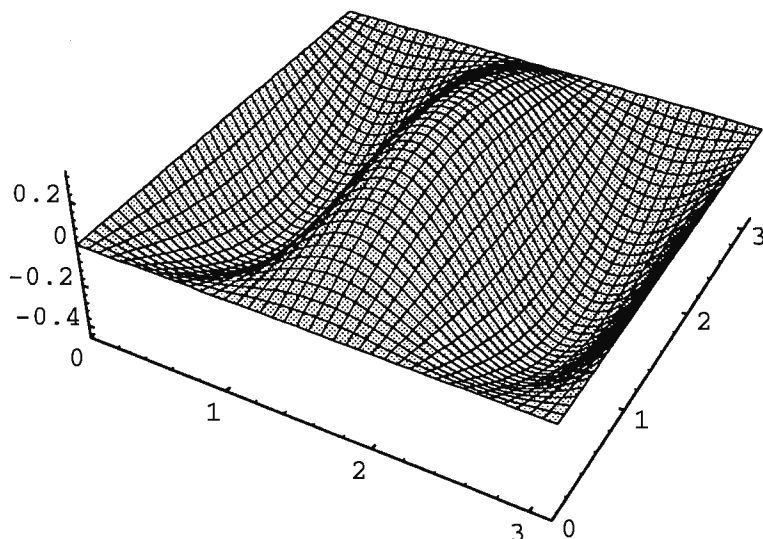
Technology

Software

Functionality



# Instrumental Innovations



Contact us for all of your NMR instrumentation needs.

North America

Otsuka Electronics USA Inc.  
800-4-OTSUKA

United Kingdom

Otsuka Electronics-Europe  
+44 1423 531

Europe

SMIS France  
+33 88 931503

Japan

JEOL Ltd.  
+(0425) 42-2185





FOR TECHNICAL INFORMATION,  
QUOTATIONS, CUSTOM SYNTHESIS,  
TO PLACE AN ORDER OR REQUEST  
A CATALOG, PLEASE CALL:  
(800) 448-9760

3858 BENNER ROAD  
MIAMISBURG, OHIO 45342  
PHONES: (513) 859-1808  
(800) 448-9760  
FAX: (513) 859-4878

**ISOTECH INC.**  
A Matheson, USA Company

## DEUTERATED NMR SOLVENTS - HANDY REFERENCE DATA

Compound Mol. Wt.	$d_4^{20}$	m.p. <sup>a</sup>	b.p. <sup>a</sup>	$\delta_H$ (mult)	$J_{HD}$	$\delta_C$ (mult)	$J_{CD}(CF)$
Acetic Acid-d <sub>4</sub> 64.078	1.12	17	118	11.53(1) 2.03(5)	2	178.4(br) 20.0(7)	20
Acetone-d <sub>6</sub> 58.08	0.87	-94	57	2.04(5)	2.2	206.0(13) 29.8(7)	0.9 20
Acetonitrile-d <sub>3</sub> 44.071	0.84	-45	82	1.93(5)	2.5	118.2(br) 1.3(7)	21
Benzene-d <sub>6</sub> 78.11	0.95	5	80	7.15(br)		128.0(3)	24
Chloroform-d 120.384	1.50	-64	62	7.24(1)		77.0(3)	32
Cyclohexane-d <sub>12</sub> 96.236	0.89	6	81	1.38(br)		26.4(5)	19
Deuterium Oxide 20.028	1.11	3.8	101.4	4.63(DSS) 4.67(TSP)			
1,2-Dichloroethane-d <sub>4</sub> 102.985	1.25	-40	84	3.72(br)		43.6(5)	23.5
Diethyl-d <sub>10</sub> Ether 84.185	0.82	-116	35	3.34(m) 1.07(m)		65.3(5) 14.5(7)	21 19
Diglyme-d <sub>14</sub> 148.263	0.95	-68	162	3.49(br) 3.40(br) 3.22(5)	1.5	70.7(5) 70.0(5) 57.7(7)	21 21 21
Dimethylformamide-d <sub>7</sub> 80.138	1.04	-61	153	8.01(br) 2.91(5) 2.74(5)	2 2	162.7(3) 35.2(7) 30.1(7)	30 21 21
Dimethyl-d <sub>6</sub> Sulfoxide 84.170	1.18	18	189	2.49(5)	1.7	39.5(7)	21
p-Dioxane-d <sub>8</sub> 96.156	1.13	12	101	3.53(m)		66.5(5)	22
Ethyl Alcohol-d <sub>6</sub> (anh) 52.106	0.91	<-130	79	5.19(1) 3.55(br) 1.11(m)		56.8(5) 17.2(7)	22 19
Glyme-d <sub>10</sub> 100.184	0.86	-58	83	3.40(m) 3.22(5)	1.6	71.7(5) 57.8(7)	21 21
Hexafluoroacetone Deuterate <sup>b</sup> 198.067	1.71	21		5.26(1)		122.5(4) 92.9(7)	(287) (34.5)
HPMT-d <sub>18</sub> 197.314	1.14	7	106(11)	2.53(2 x 5)	2(9.5)	35.8(7)	21
Methyl Alcohol-d <sub>4</sub> 36.067	0.89	-98	65	4.78(1) 3.30(5)	1.7	49.0(7)	21.5
Methylene Chloride-d <sub>2</sub> 86.945	1.35	-95	40	5.32(3)	1	53.8(5)	27
Nitrobenzene-d <sub>5</sub> 128.143	1.25	6	211	8.11(br) 7.67(br) 7.50(br)		148.6(1) 134.8(3) 129.5(3) 123.5(3)	24.5(p) 25 26
Nitromethane-d <sub>3</sub> 64.059	1.20	-29	101	4.33(5)	2	62.8(7)	22
isoPropyl Alcohol-d <sub>8</sub> 68.146	0.90	-86	83	5.12(1) 3.89(br) 1.10(br)		62.9(3) 24.2(7)	21.5 19
Pyridine-d <sub>5</sub> 84.133	1.05	-42	116	8.71(br) 7.55(br) 7.19(br)		149.9(3) 135.5(3) 123.5(3)	27.5 24.5(g) 25
Tetrahydrofuran-d <sub>8</sub> 80.157	0.99	-109	66	3.58(br) 1.73(br)		67.4(5) 25.3(br)	22 20.5
Toluene-d <sub>8</sub> 100.91	0.94	-95	111	7.09(m) 7.00(br) 6.98(m) 2.09(5)	2.3	137.5(1) 128.9(3) 128.0(3) 125.2(3) 20.4(7)	23 24 24(p) 19
Trifluoroacetic Acid-d <sup>c</sup> 115.030	1.50	-15	72	11.50(1)		164.2(4) 116.6(4)	(44) (283)
2,2,2-Trifluoroethyl Alcohol-d <sub>3</sub> <sup>d</sup> 103.059	1.45	-44	75	5.02(1) 3.88(4 x 3)	2(9)	126.3(4) 61.5(4 x 5)	(277) 22(36)

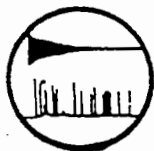
<sup>a</sup>Melting and boiling points (in °C) are those of the corresponding light compound (except for D<sub>2</sub>O) and are intended only to indicate the useful liquid range of the materials. The multiplicity br indicates a broad peak without resolvable fine structure, while m denotes one with fine structure.

<sup>b</sup> $\delta_F(CFCl_3)$  82.6(1)

<sup>c</sup> $\delta_F(CFCl_3)$  76.2(1)

<sup>d</sup> $\delta_F(CDCl_3)$  77.8(5),  $J_{FD}$  1.2





**SOPHISTICATED INSTRUMENTS FACILITY**  
(Sponsored by the Department of Science & Technology, Government of India)  
**INDIAN INSTITUTE OF SCIENCE**  
BANGALORE-560 012 INDIA



October 19, 1995  
(received 11/13/95)

Dr.B.L. Shapiro  
The NMR Newsletter  
966 Elsinore Court  
Palo Alto, CA 94303  
USA

**From spectral editing to extracting dipolar couplings in partially oriented systems**

Dear Barry,

We were interested in finding a suitable editing sequence for identifying carbon resonances in static liquid crystal samples in their nematic phases. We realised that the dipolar dephasing sequence of Opella and Frey<sup>1</sup> would not work, since in the case of the oriented liquid crystal sample the carbons with attached protons have possibly resolved dipolar couplings with a small line-width and hence do not dephase fast enough. On the other hand, we observed that the cross-depolarisation sequence proposed by Zumbulyadis<sup>2</sup> works well for such samples (Fig.1).

In the course of optimising the depolarisation time for p-methoxy benzylidene p'-n-butylaniline (MBBA), we noticed that the intensities of the carbon peaks undergo an oscillatory change superposed on a monotonic change both during cross-polarisation and cross-depolarisation (Fig.2). These are in fact the transient oscillations in cross polarisation reported by Muller et al. on a single crystal of ferrocene<sup>3</sup>. The oscillation frequencies can be employed to provide the proton-carbon dipolar couplings and the corresponding liquid crystal order parameters<sup>4</sup>. A two dimensional experiment with the pulse sequence shown (Fig.3) has also been tried. The experiment provides the above information in one go and hence is more convenient (Fig.4).

**References**

1. S.J. Opella and M.H.Frey, J. Am. Chem. Soc., 101, 5884 (1979).
2. N. Zumbulyadis, J. Chem. Phys. 86, 1162 (1987).
3. L. Muller, Anil Kumar, A. Baumann and R.R. Ernst, Phys. Rev. Lett., 32, 1402 (1974).
4. R. Pratima and K.V. Ramanathan, J. Magn. Reson. A (In Press).

Regards,

*K.V. Ramanathan*

K.V. Ramanathan

*C.L. Khetrapal*

C.L. Khetrapal



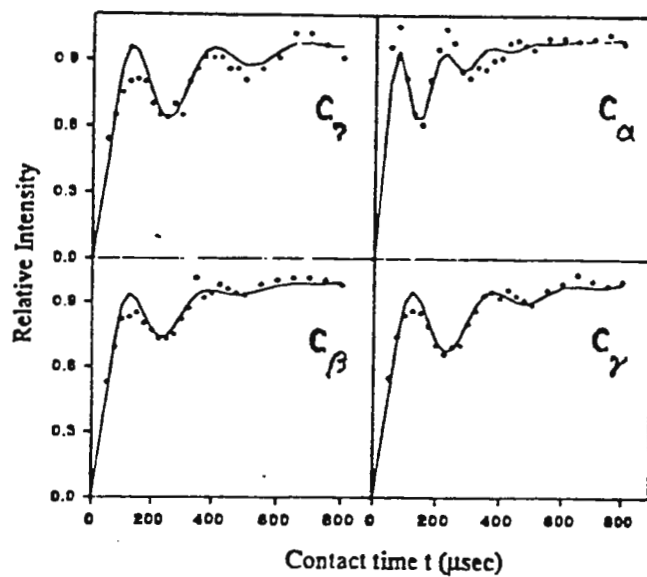
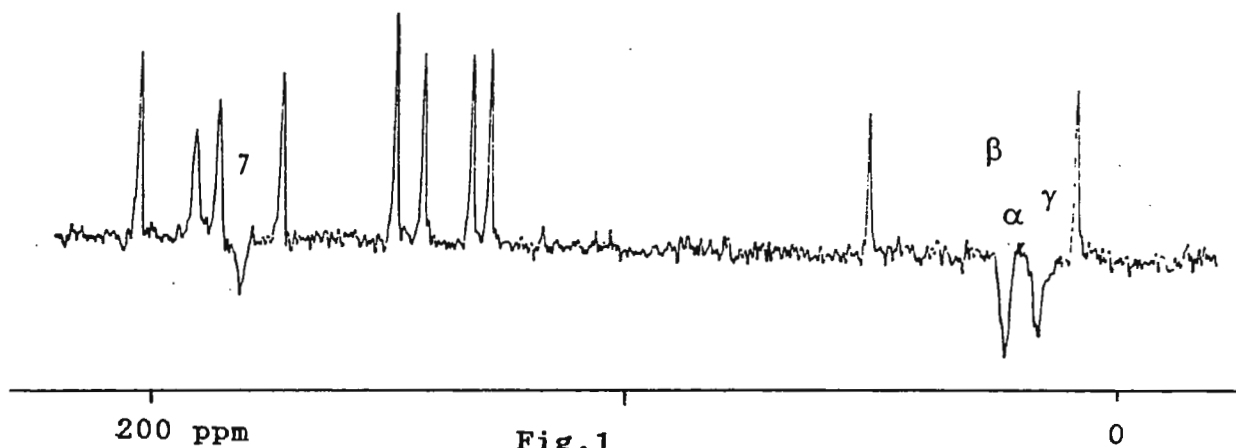
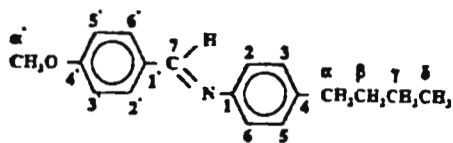


Fig. 2

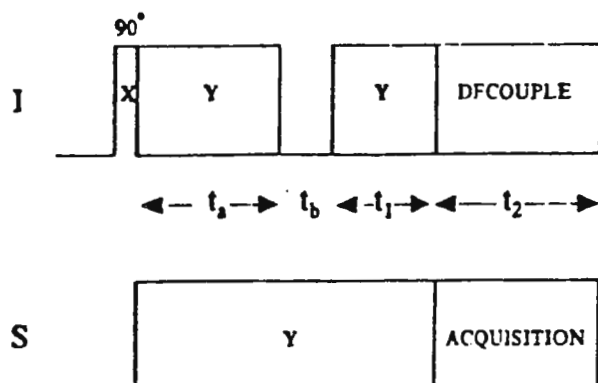


Fig. 3

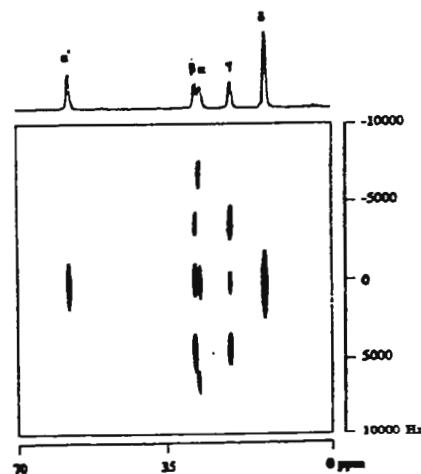
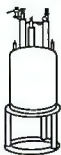
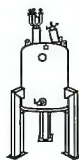
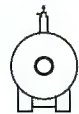


Fig. 4

# Reflecting our commitment to quality all year round



Oxford Instruments continues to lead the field with innovative technology that has become the benchmark of NMR magnet excellence.

With over 30 years at the forefront of NMR magnet technology and over 4000 successful installations worldwide, our products continue to be the preferred choice for NMR specialists.

From 100 MHz to 900 MHz and beyond, Oxford Instruments have established an enviable reputation for delivering products which are designed to provide superb performance year after year.

Whether you need a custom approach, or a specific application from one of our standard vertical or horizontal bore magnet systems, Oxford Instruments have the skills and expertise to give you the right solutions-with a global support service designed to respond to your demands.

**A very happy Christmas and a prosperous new year from everyone at...**

***Oxford Instruments.***



## OXFORD

**Oxford Instruments  
NMR Instruments**

# The Oxford Instruments Heritage

Oxford Instruments are the pioneers of NMR magnet systems and associated cryogenic technology. After more than 30 years, we are still leading the way maintaining our worldwide reputation for transforming scientific ideas into usable, practical technology:

- Oxford Instruments were the first company to introduce NMR quality super-conducting magnets at 400, 500, 600 and 750 MHz.

- We designed and built the world's first compact superconducting storage ring for X-ray lithography.

- 20 Tesla magnets are routinely produced for physics research.

Making this happen are the people of Oxford Instruments, their expertise and dedication makes them our greatest asset and a unique resource for our customers.

Our accumulated knowledge and experience is unparalleled and some of the best minds in research technology are consistently working in partnership with our customers, exploring new techniques and setting new standards in the design and manufacture of specialist

research products.

But it does not stop there; supporting our customers day to day, and around the world, is a team of engineers and technical specialists. Always on hand, to keep our products fully functional and equipped with the latest refinements.

New products such as the Oxford NMR<sup>TM</sup> are practical examples of our innovation so you can be sure of Oxford Instruments commitment to providing the very best in people and products for many years to come.

## Standard specifications

Magnetic field Strength ('H-MHz)	Room Temperature Bore Diameter (mm)	Field Stability ('H-Hz/Hour)	Maximum Helium Refill Interval (Days)	Minimum Operational Ceiling Height (m)
750	51	15	60	3.8
600	51	10	120	3.4
500	51	10	150	3.2
400	54	8	365	2.8
360	54	8	365	2.8
300	54	3	365	2.8
270	54	2.7	365	2.8
200	54	2	365	2.8
100	54	1	365	2.8
500	89	15	120	3.4
400	89	10	180	2.8
360	89	10	365	2.8
300	89	3	365	2.8
270	89	2.7	365	2.8
200	89	2	365	2.8
100	110	1	119	2.8

**We would be delighted to discuss your custom specification requirements for any specialist systems. For more information please contact your local Oxford Instruments sales and service organisation.**

### UK

Oxford Instruments  
NMR Instruments,  
Osney Mead, Oxford OX2 0DX,  
England  
Tel: +44 (0) 1865 269500  
Fax: +44 (0) 1865 269501

### Germany

Oxford Instruments GmbH  
Kreuzberger Ring 38,  
Postfach 4509, D-6200 Wiesbaden,  
Germany  
Tel: (611) 76471  
Fax: (611) 764100

### USA

Oxford Instruments Inc.  
130A Baker Avenue, Concord,  
MA 01742, USA  
Tel: (508) 369 9933  
Fax: (508) 369 6616

### France

Oxford Instruments SA  
Parc Club-Orsay Universite,  
27, rue Jean Rostand,  
91893 - Orsay Cedex,  
France  
Tel: (1) 6941 8990  
Fax: (1) 6941 8680

### Japan

Oxford Instruments K.K.  
8F, Second Funato Building,  
1-11-11, Kudankita,  
Chiyoda-ku, Tokyo 102  
Japan  
Tel: (3) 3264-0551  
Fax: (3) 3264-0393 · 0626

Oxford Instruments Inc.  
West Regional Office,  
331c Lakeside Drive,  
Foster City, California 94404  
USA  
Tel: (415) 578 0202  
Fax: (415) 578 9018

# OXFORD

### Oxford Instruments, NMR Instruments

Osney Mead  
Oxford OX2 0DX, England  
Telephone +44 (0) 1865 269500 Fax +44 (0) 1865 269501





MAGNETIC RESONANCE UNIT  
Veterans Administration Medical Center  
4150 Clement Street (114M)  
San Francisco, CA 94121  
Tel: (415) 221-4810 x4803  
Fax: (415) 668-2864  
E-mail: nschuff@itsa.ucsf.edu

November 14, 1995  
(received 11/17/95)

Dr. Bernard L. Shapiro  
The NMR Newsletter  
966 Elsinore Court  
Palo Alto, CA 94303

re: Multislice  $^1\text{H}$  Magnetic Resonance Spectroscopic Imaging to Study Dementia

Dear Dr. Shapiro,

We have been using  $^1\text{H}$  magnetic resonance spectroscopic imaging (MRSI) in our laboratory for several years to study Alzheimer's disease (AD) [1]. So far, however, data acquisition was constrained to a box-shaped region within the brain, sufficient away from the surface cortex, and without multislice capability. This was necessary to minimize contamination of  $^1\text{H}$  metabolite spectra from intense lipid resonances, primarily from lipids of subcutaneous tissue. Recently, we have implemented a new version of multislice MRSI on our clinical 1.5T MR scanner (VISION<sup>TM</sup>, Siemens) which enables us to observe  $^1\text{H}$  metabolite resonances from the entire brain, including surface cortex, an area which is believed to be affected very early in AD.

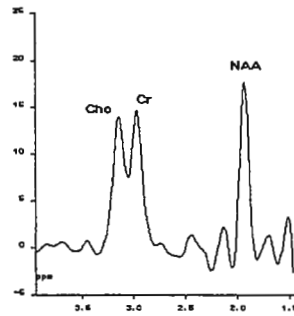
Multislice MRSI has been reported by several groups, but most strategies employ outer volume suppression pulses to reduce the intensity of the lipid signal. Unfortunately, these pulses also saturate spins of the surface grey matter of the brain, making quantitation of  $^1\text{H}$  metabolites difficult. We have developed a technique for multislice  $^1\text{H}$  MRSI which does not utilize outer volume suppression pulses. Lipid removal is accomplished entirely by postprocessing. This technique takes advantage of the method suggested by Hu et. al. [2] and the Papoulis-Gerchberg algorithm for data reconstruction by k-space extrapolation [3]. This method accomplished to reduce the intensity of the lipid signal by about 85%, sufficient to obtain a well resolved resonance line from NAA, as well as from choline (Cho) and creatine (Cr), the two other major peaks in brain spectra.

Using this approach of multislice MRSI, we have been able to acquire  $^1\text{H}$  metabolite MR spectra from the entire brain of AD patients. A metabolite image of NAA through temporal lobes and hippocampi from a 81 years old AD patient is shown below. This image was obtained by line-fitting of the NAA resonance and subsequent integration. Also shown is the proton image (MRI) from the same brain region. To our knowledge, this is the first time that NAA has been observed from the entire region of the temporal lobes of an AD brain, including the lateral temporal association cortices (positions (c) and (d) indicated in the MRI). The four metabolite spectra shown below and selected from temporal association cortices and hippocampi (a,b) demonstrate

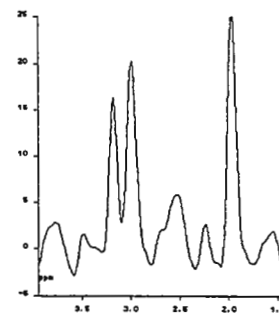
the excellent spectral resolution achieved. Total acquisition time of the experiment was 30 minutes, including the selection of 4 slices (each 1.5cm thick), TR/TE values of 1800/140ms, and 36 x 36 phase-encoding steps yielding a nominal pixel resolution of the NAA image of 8 x 8 mm<sup>2</sup>. We anticipate that multislice <sup>1</sup>H MRSI will be very helpful to determine regional patterns of metabolite changes in AD which eventually might aid the early detection and diagnosis of this devastating disease.



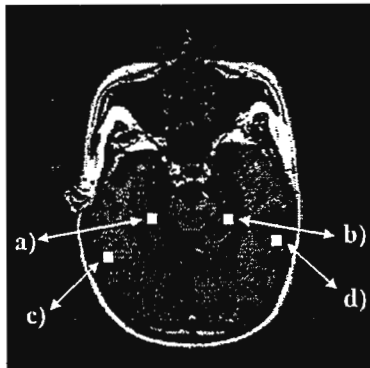
NAA Metabolite Image



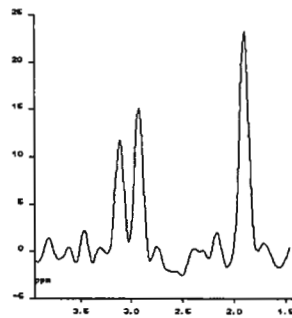
(a) from right



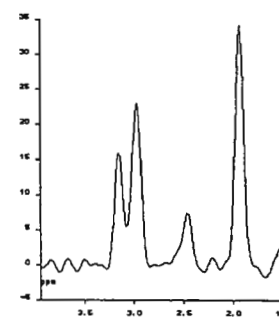
and (b) left hippocampus



MRI



(c) from right



and (d) left temporal association cortex

1. MacKay, S., Ezekiel, F., Di Sciafani, V., Gerson, J., Meyerhoff, D.J., Norman, D., Fein, G., and Weiner, M.W. Combining MRI segmentation and <sup>1</sup>H MR spectroscopic imaging in the study of Alzheimer's disease, subcortical ischemic vascular dementia and elderly controls. *Radiology* (In Press).
2. Hu, M. Patel, and K. Ugurbil. A new strategy for spectroscopic imaging. *J. Magn. Reson. B*, **103**, 30-38 (1994).
3. Haupt, C. I., Schuff, N., Weiner, M. W., Maudsley A. A.: Lipid removal in <sup>1</sup>H spectroscopic imaging by data extrapolation. (submitted)

Sincerely yours

Norbert Schuff

Christine I. Haupt

Michael W. Weiner

Andrew A. Maudsley

# Scale the Heights in NMR Magnet Performance

## *Introducing the BRUKER SPECTROSPIN 600 MHz /52 mm High Resolution NMR Magnet*

### **BRUKER SPECTROSPIN**

SPECTROSPIN is the largest manufacturer of superconducting NMR magnets with over 30 years of experience in design and manufacturing. The quality of SPECTROSPIN magnets is second to none. Exceptional specifications are delivered with each system.

Our R&D group of scientists and engineers use advanced computational tools for magnetic field calculations, structural analysis, conductor design, quench protection and electrical design.

SPECTROSPIN uses state of the art production techniques: micro processor controlled winding, computer controlled furnace for the reaction of Niobium-Tin wire, micro processor controlled impregnation, advanced jointing technology, NMR based testing for magnet quality control.

Many SPECTROSPIN superconducting magnets built in the late 70's and early 80's are still on field and providing quality data and dependable service.



**ISO 9001  
CERTIFIED**

## **Main Features**

- Ultra large volume with outstanding field homogeneity provides excellent resolution and non-spinning lineshape; also, this permits the use of larger and more dilute samples.
- Lowest drift rates.
- Advanced anti-vibration stand system integrated with the cryostat supported at its center of gravity for better performance. Each of the three support posts is connected to the other two using horizontal bars, making alignment much easier.
- Helmholtz helium vibration dampers.
- Extremely low helium evaporation rates.
- Electronic atmospheric pressure device to stabilize the field drift and helium boil-off when changes in atmospheric pressure occur.
- Reduced minimum ceiling height installation requirements.



*Comprehensive Support for Innovative Systems*



# SPECIFICATIONS

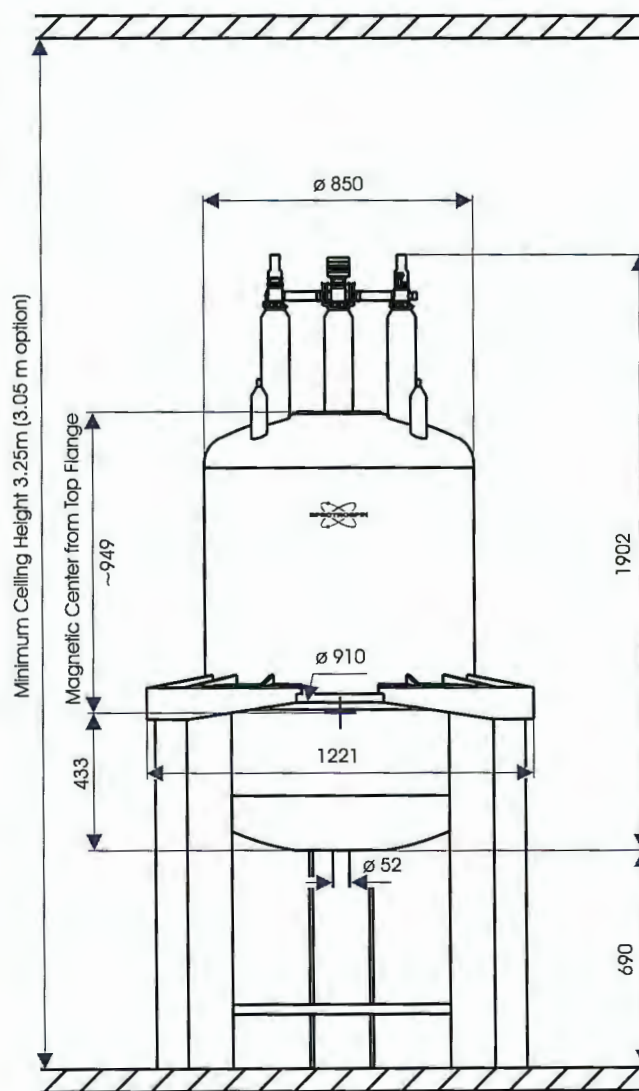
## MAGNET

Central Field	14.1 T
NMR Frequency	600 MHz
Field Drift	< 9 Hz/hr
Cryo-shims	z, z <sup>2</sup> , x, y, xz, yz, xy, x <sup>2</sup> -y <sup>2</sup>
Axial range with field homogeneity better than 10 ppm (w/o RT shimming)	60 mm
Resolution FWHM, ODCB 5mm spinning	< 0.25 Hz
Non-spinning lineshape 5mm CHCl <sub>3</sub> non-spinning	at 0.11% < 6 Hz *
	at 0.55% < 12 Hz *
Spinning Sidebands	< 1%

## CRYOSTAT

Helium Evaporation Rate	< 35 ml/hr
Helium Refill Volume	126 l
Helium Hold Time	> 150 days
Nitrogen Evaporation Rate	< 340 ml/hr
Nitrogen Refill Volume	163 l
Nitrogen Hold Time	> 20 days
Minimum Ceiling Height	3.25 m
Reduced Minimum Ceiling Height (with special equipment)	3.05 m

### 600 MHz / 52 mm Magnet



Dimensions in millimeters unless stated otherwise.

\* Typical values obtained with the BOSS II™ shim system.

### USA

**BRUKER SPECTROSPIN, INC.**  
 19 Fortune Dr., Manning Park  
 Billerica, Mass. 01821  
 Tel. (508) 667 - 9580  
 Fax. (508) 667 - 3954



<http://www.bruker.com>

### Switzerland

**SPECTROSPIN AG**  
 Industriestrasse 26  
 CH-8117 Fallanden  
 Tel. (41) 1 825 91 11  
 Fax. (41) 1 825 96 96

CEA, DEPARTEMENT de RECHERCHE FONDAMENTALE  
 sur la MATIERE CONDENSEE  
 SESAM/SCPM  
 17, rue des Martyrs  
 38054 GRENOBLE CEDEX 9, FRANCE

October 4, 1995  
 (received 10/30/95)

Dr. B.L. Shapiro  
 The NMR Newsletters  
 966 Elsinore Court  
 Palo Alto, CA 94303  
 USA

Dear Dr. Shapiro,

### Non-Selective $T_1$ Relaxation Times Measurements by the Newly Developed IR-TOCSY

Longitudinal relaxation times are usually determined by the classical  $^1\text{H}$  non-selective inversion-recovery (IR) sequence. Yet this sequence is of limited interest in molecules which overcrowded 1D spectra.

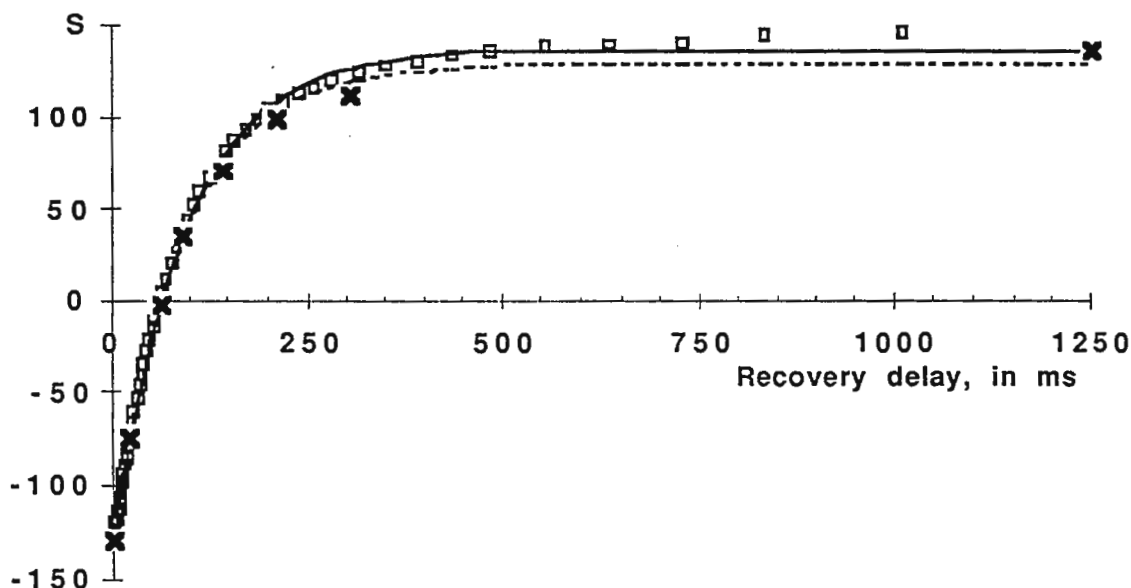
The IR-COSY sequence<sup>1</sup> takes advantage of the better resolution of 2D spectra to measure non-selective  $T_1$  values. This sequence consists of the conventional inversion-recovery followed by a COSY sequence. The recovery delay is incremented in order to obtain a serie of 2D experiments. The intensity of a cross peak between protons H1 along F1 and H2 along F2 is a function of the IR delay and of the non-selective  $T_1$  value of H1 but not of H2<sup>1</sup>.

The IR-TOCSY was built by substituting the COSY sequence by a TOCSY<sup>2</sup> one. The IR-TOCSY combines the advantages of IR-COSY and TOCSY, mainly increased resolution and cross peaks in phased pure absorption mode. Furthermore, in the case of paramagnetic proteins, the broad antiphase correlation peaks often cancel out in a COSY-type experiment.

The applicability of the IR-TOCSY to measure the non-selective  $T_1$  of paramagnetic reduced *Chromatium vinosum* high potential ferredoxin<sup>3</sup> has been demonstrated by comparison with 1D inversion-recovery sequence.

The intensity of 1D signals and 2D correlation peaks was fitted with the function :  $S = A \left( 1 - 2B \exp \left( -\frac{\text{delay}}{T_1} \right) \right)$

The results obtained with the NH of Ile 71 are shown.



The squares and the crosses correspond to the values obtained from 1D IR and IR-TOCSY experiments respectively. The continuous and the dashed lines are the corresponding fits.

Non-selective  $T_1$  values of 94 ms and 92 ms were deduced from the 1D IR and IR-TOCSY experiments respectively. These values were in good agreement for all the protons studied, with less than 10 % error, which is the classical estimated error.

## REFERENCES

- 1 - Arseniev A. S. , Gobol A. G. and Bystrov V. F. (1986) J. Magn. Reson. 70, 427-435
- 2 - Bax A. and Davis D. G. , J. Magn. Reson. 65 (1985) 355-360
- 3 - Gaillard J. , Albrand J.-P., Moulis J.-M. and Wemmer D. E. (1992) Biochemistry 31, 5632-5639

Sincerely yours,

Huber J. G.

Gaillard J.

This work was carried out in collaboration with Dr. J.-M. Moulis, CEA, DBMS, Laboratoire de Métalloprotéines, Grenoble, France

P.S. Please credit this contribution to the account of Dr. Philippe Vottero.



# Cambridge Isotope Laboratories

**CIL** would like to thank our loyal customers for their patronage throughout the year. To show our appreciation for your business, we would like to extend special savings to you.

Place your order before **December 31, 1995**  
and receive the following discounts:

Order **2 x Catalog quantity**  
and receive **10% off** catalog prices

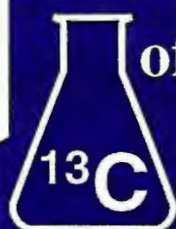
Order **3 x Catalog quantity**  
and receive **15% off** catalog prices

To contact your CIL sales representative within the  
United States call 1-800-ISOTOPE (800-476-8673)  
and in Canada call 1-800-668-2181.

**Customer Satisfaction**  
**is our #1 Goal**



The World's Leading Supplier



of Stable Isotope Labeled

Compounds



CIL has the most complete inventory  
of stable isotope labeled compounds...

NMR Solvents & Reagents, Amino Acids,  
Gases, Enriched Cell Growth Media,  
Sugars, Nucleosides, Lipids, Fatty Acids,  
<sup>13</sup>C Breath Test Substrates, Steroids, Polymers,  
and Environmental Standards.

*Please call for product information  
and your free 1994-1995 catalog!*



USA: 800-322-1174  
508-749-8000

Canada: 800-643-7239

Fax: 508-749-2768

e-mail: [cilsales@isotope.com](mailto:cilsales@isotope.com)



*We invite your requests for custom syntheses.*

**CAMBRIDGE ISOTOPE LABORATORIES**

**50 Frontage Road, Andover, Massachusetts 01810 USA**



Stefano Caldarelli  
 Services RMN - Section de Chimie  
 Université de Lausanne -BCH  
 CH-1015 Dorigny  
 Switzerland

TEL: ++41 21 692 3802 / 3803  
 FAX: ++41 21 692 3855  
 E-Mail: Stefano.Caldarelli@unil.ch

### Pure-phase selective excitation

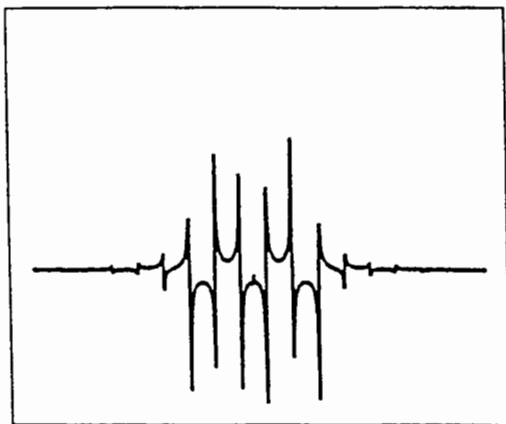
Lausanne, Tuesday, October 31, 1995 (received 11/4/95)

Dear Dr. Shapiro,

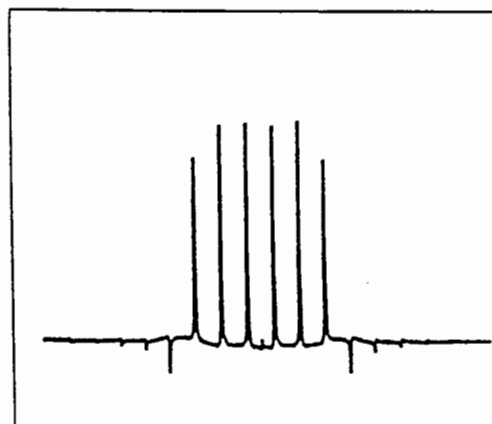
Selective excitation has been used in NMR as a useful tool to achieve accurate measurements in complex systems. Typical advantages of selective methods are: the possibility of limiting the duration of the time domains in a multidimensional experiment; reduced high-dimension experiments can be conceived.; selective removal of unwanted effects (refocussing of spin-diffusion, decoupling).

On the other hand, the technique is not flawless. One of the problems that have to be faced is the linear phase distortion that is introduced in the excitation window as a function of the offset. This is a general effect for symmetric excitation pulses and can be understood in terms of the shift theorem of the Fourier Transform. In fact, the complex FT of a symmetric pulse is a pure real function in the frequency domain only if the origin of the time is set in the middle of the excitation pulse. A shift in the time domain corresponds to a linear phase gradient in the frequency domain. Therefore, the linear phase gradient observed in the NMR experiment is due to the choice of the origin of time (i.e. the beginning of the acquisition) at the end of the pulse. The effect is then ubiquitous but much more dramatic in the case of selective excitation, where the long pulses used in order to achieve the desired window of excited frequencies are comparable in length to the dwell time.

Excitation schemes designed to prevent this drawback have been proposed over the years. They include projection methods, that only keep the magnetization with the desired phase or self-refocussing pulses, that drives the magnetization along specific paths in order to amount to good excitation and no offset dependent phase gradient as an overall effect.



Excitation profile of a sinc-shaped DANTE pulse train



Excitation profile of a sinc-shaped DANTE pulse train with retro-active acquisition



Recently, we proposed an alternative methodology that allows to achieve "pure-phase" excitation using arbitrary symmetric shaped pulses. The scheme consists in altering a "normal" NMR experiment by regressing the origin of time back to the middle of the pulse.

Experimentally this is implemented by "chopping" a regular shaped pulse, in order to create what can be regarded as a shaped DANTE pulse train. The usual requirements for the pulse/delay ratio typical of DANTE are observed. The "windows" in the pulse (i.e. the periods with RF off) can be used to acquire points before the end of the pulse, a special case being the middle of the pulse.

We decided to call this technique *pure-phase achieved by retroactive acquisition in DANTE-implemented selective excitation (PARADISE)*, noticing that it constitutes perhaps the last step on the path of DANTE ...

The effect of implementing this particular scheme are shown in the figure for a sinc pulse shape, but other symmetrical shapes may be used according to anyone's right to choose their own PARADISE.

Best regards,

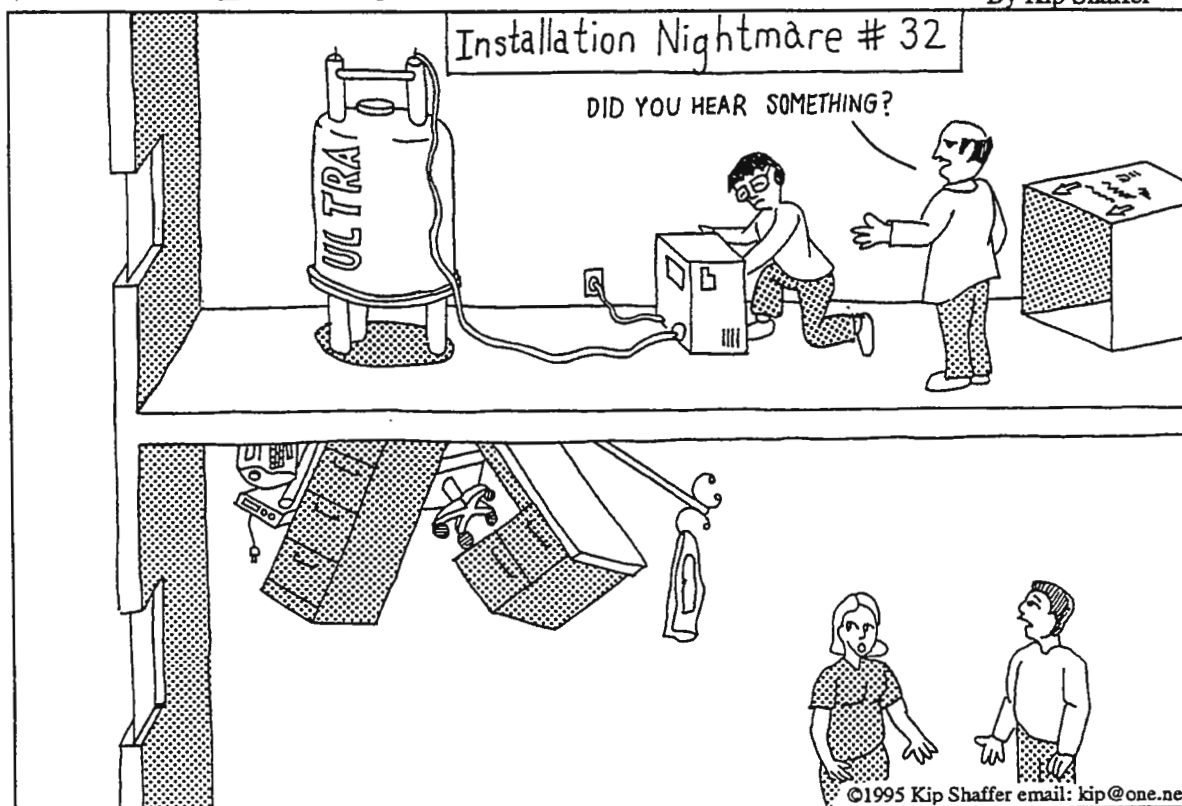
  
Stefano Caldarelli

(1) S. Caldarelli, A. Lesage and L. Emsley, Journ. Magn. Reson. 116,129 (1995)

Please credit this contribution to the account of Prof. A. Merbach

## Field of Dreams

By Kip Shaffer





**EXPLORE THE ALTERNATE ROUTE...!**

# **QUALITY REFURBISHED NMRs**

**BRUKER . JEOL . VARIAN**

**PERMANENT MAGNETS . ELECTRO MAGNETS . CRYO MAGNETS**

\*\*\*\*\*

**CURRENTLY IN STOCK:    BRUKER NR-80, AM-300, AM-400**

**VARIAN EM-360A, EM-360L,  
EM-390, XL-200, VXR-400**

**JEOL FX-90Q, GX-270**

**FOR FURTHER DETAILS CALL: (708) 913-0777**

**International Equipment Trading Ltd.  
960 Woodlands Parkway, Vernon Hills, IL 60061  
FAX: (708) 913-0785**



# Call Now for the Best Value!

New and Reconditioned  
Analytical Instruments

## INVENTORY UPDATE

### X-RAY:

ARL 8680 Fluorescence  
Cordell MXR-14 X-ray film processor  
Stoe, Bragg-Brentano diffractometer  
Tracor TX-5000

### GAS CHROMATOGRAPHS:

Carlo Erba FID/NPD + A/S  
HNU 311 PID  
HP 5880 FID/TCD + 7672 A/S  
HP 5880 TCD/FPD  
HP 5880 dual FID  
HP 3393 integrator  
Hitachi D2000 integrator  
O.I. 4460A purge and trap  
PE 8500 FID/NPD/ECD  
PE 8320 FID  
Shimadzu C-R3A integrator  
Spectra Physics 4270 integrator  
Tekmar LSC-II purge and trap  
w/ ALS-10 autosampler  
Varian 3400 FID/NPD  
Varian 3700 dual FID capillary  
Varian 3700 ECD/FID capillary  
Varian Vista 6000 PID/FID w/ P&T  
Varian Vista 6000 dual ECD  
Varian 8035 autosampler

### H.P.L.C.:

Beckman 112 solvent delivery w/ 421  
gradient pump & controller, 340 organizer  
Dionex 2010i ion chromatograph  
HP 1040M diode array detector  
HP 1090M HPLC w/ Pascal workstation, A/S  
& diode array detector  
Waters 600 multi solvent system  
Waters 710B Wisp autosampler  
Waters 712B Wisp autosampler  
Waters 510 pump  
Waters 501 pump  
Waters 490 multiwavelength detector  
Waters Delta-prep 3000  
Waters 481 uv-visible detector  
Waters ILC-I ion chromatograph  
Waters Auto-500 Prep-LC

### MASS SPECTROMETERS:

Finnigan 5100 GC/MS  
Finnigan TSQ-70B triple quad  
Finnigan Incos-50B  
Finnigan TSQ-700 triple quad  
Finnigan 806A Ion Trap w/Varian 3400 GC

HP 5970B w/ HP 5890A GC  
HP 5971 w/ DOS, UNIX, jet separator, 7673 A/S  
HP 5987 GC/MS w/ particle beam  
HP 5988 w/ 7673 A/S  
VG 70-250  
VG ZAB 1F system

### UV-VIS:

Beckman DU-50 w/Kinetics  
Beckman DU-7 w/ A/S  
Beckman DU-8B w/ Gel Scanner  
Varian 2290

### ATOMIC ABSORPTION:

ARL 3510 ICP  
Baird PS-4 ICP  
Baird PSX-18 ICP w/ IBM PS/2  
IL Video 22  
Jobin Yvon JY-70 Plus ICP  
Leeman Labs PS-950 ICP  
Leeman Labs PS-1 ICP  
PE 603 w/ HGA-2100 + EDL  
PE 2380  
PE 5000 w/ HGA-500 & AS-40  
PE Zeeman 5000  
PE Zeeman 3030  
PE Zeeman 4100ZL  
PE HGA-400  
PE HGA-500 w/ AS-40 A/S  
PE HGA-600 w/ AS-60 A/S  
PE AS-51 autosampler  
PE 6500 ICP  
PE Plasma 2000  
PE Plasma 400  
Spectro FMA-05 ICP  
Varian Spectra 40 w/ GTA-96 & PSC-56  
Varian Spectra 30  
Varian 975 w/ GTA-95 & A/S  
Varian 475 w/GF & A/S

### DISPERSIVE IR:

PE 683  
PE 781  
PE 710B  
PE 1421  
PE 983G

### FT-IR:

Bio-Rad FTS-60 QC  
Mattson Cygnus 100 w/ IR plan microscope  
Nicolet 20SX-B  
Nicolet 740  
PE1850 w/ IR plan microscope

### RESONANCE SPECTROMETERS:

Bruker NR-80 NMR  
Bruker AM-300 NMR  
Bruker AM-400 NMR  
JEOL FX-90Q NMR  
JEOL GX-270 NMR  
Varian EM-390 NMR  
Varian EM-360L NMR  
Varian VXR-400 NMR  
Varian XL-200 NMR  
Varian XL-400 NMR

### ELECTRON MICROSCOPES:

Cambridge 120 SteroscanSEM  
Hitachi S-520 SEM w/KeveX  
Hitachi S-2300 SEM w/ KeveX  
ISI SS 40 SEM  
Hitachi 600 AB TEM w/ KeveX  
JEOL 1200 EX TEM w/ KeveX-Delta  
Phillips CM-12 TEM w/ EDAX-9900

### BIOTECHNOLOGY:

Applied Biosystems (ABI) Protein Sequencer 477A  
w/120A PTH  
ABI DNA Synthesizer 380B  
ABI Peptide Synthesizer 430A  
ABI Separation system 130A  
Beckman L8-80 ultra centrifuge  
Coulter EPICS C Flow Cytometer  
Sorvall RC-2B  
Sorvall RC-3B  
Sorvall RC-5B  
Sorvall OTD-65B ultra centrifuge

### ELEMENTAL ANALYZERS:

Antek 707C nitrogen analyzer  
Dohrmann DC-80 TOC analyzer  
Dohrmann DX-20A TOX analyzer  
Leco CS-244  
Leco SC-132 auto sulfur determinator  
Leco DH-103 hydrogen analyzer  
PE 240C CHN

### MISCELLANEOUS:

A.O. model 820 microtome  
Fisher 490 coal analyzer  
Kjeldahl 24-position apparatus  
NELSON Lab automation system  
Nova Analytical ISE analyzer  
PE LS-3 flourimeter  
PE DSC-4  
Rheometrics RDS-7700 II  
Technicon Auto Analyzer II



Reconditioned equipment carries a 90-day warranty for parts and labor unless  
otherwise noted. The availability of all equipment is subject to prior sale.

**International Equipment Trading, Ltd.**

960 Woodlands Parkway • Vernon Hills, Illinois 60061 (708) 913-0777 Fax (708) 913-0785

SERVING THE  
SCIENTIFIC COMMUNITY





STIM-SRV  
INRA THEIX  
63122 Ceyrat - FRANCE

Professor B. L. SHAPIRO  
966 Elsinor Court  
Palo Alto  
California 94303 - Etats Unis

Dear Dr Shapiro

Theix, 7 November 1995  
(received 11/20/95)

## THE MAGNETIC FIELD DEPENDENCE OF WATER PROTONS TRANSVERSE RELAXATION IN GELATIN

To characterize water-gelatin interactions, the transverse water proton relaxation rates ( $1/T_2$ ) were measured on water-gelatin solution at two Larmor frequencies (20 and 400 MHz). The CPMG pulse sequence was used with a 2 ms-interpulse spacing. Gelatin concentration was 10% (w/w) and the pH was adjusted to 6. Samples were thermostated at three sol state temperatures.

At 20 MHz,  $1/T_2$  increases with the inverse of absolute temperature while it decreases at 400 MHz. These results can be explained by two dynamic processes. In our condition of long interpulse spacing,  $\frac{1}{T_2} = \frac{P_a}{T_{2a}} + \frac{P_b}{T_{2b}} + \frac{P_b(\Delta\delta\omega)^2}{k_b}$  where  $T_{2i}$  is the relaxation time in the site  $i$ ,  $P_i$  is the population in the site  $i$  and  $1/k_b$  is the lifetime in the site  $b$  and  $(\Delta\delta\omega)$  is the chemical shift difference between the two sites (1). At high frequency,  $1/T_2$  depends on the chemical exchange because  $\frac{(\Delta\delta\omega)^2}{k_b} \gg \frac{1}{T_{2b}}$ , while at 20 MHz,  $(\Delta\delta\omega)^2$  is 400 times less than at 400 MHz and  $\frac{1}{T_{2b}}$  should also decrease. So dipole-dipole interactions are prevailing.

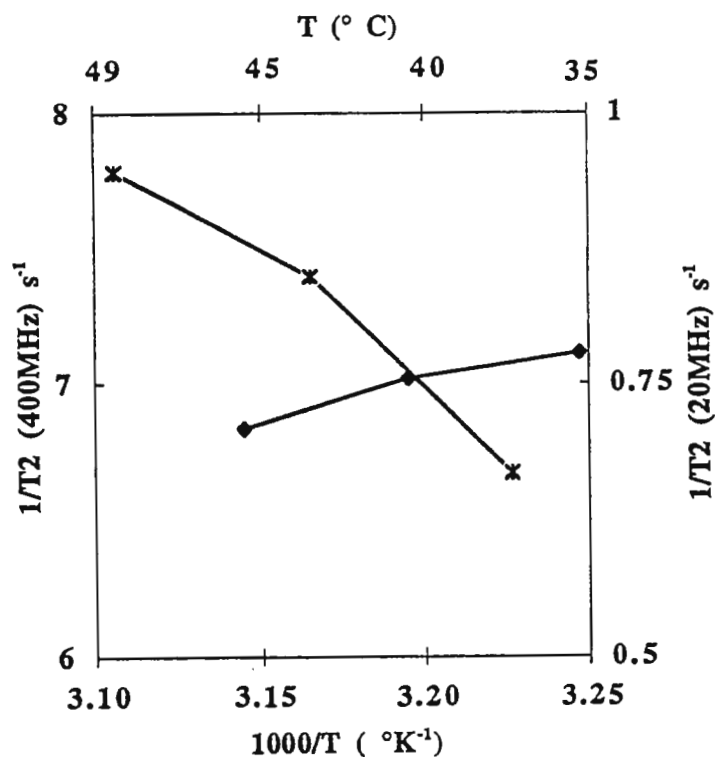
Sincerely yours,

A. TRAORE

L. FOUCAT

J.P. RENOU

(1) Carver J.P. & Richards R.E. (1972) *J. Magn. Reson.* 6; 89.



Transverse water proton relaxation rate  $1/T_2$  ( $s^{-1}$ ) plotted versus reciprocal temperature for gelatin 10% at 20MHz (♦) and 400MHz(\*).

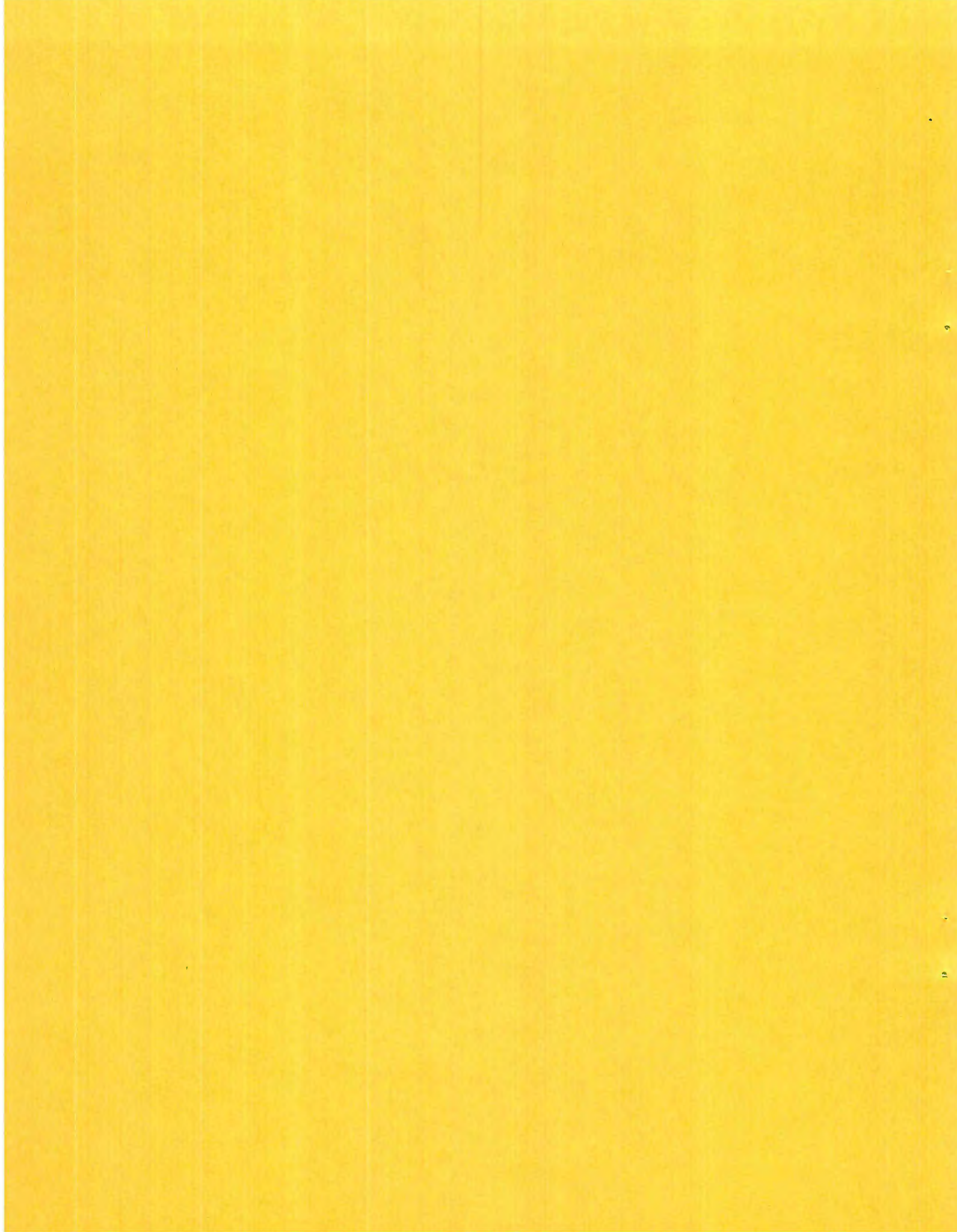
- Continued from page 40.

Table 1:

ATOM	cal_T1(sec)	exp_T1(sec)	ATOM	cal_T1(sec)	exp_T1(sec)
A3H2	6.33	12.3	C2H6	1.80	-
A5H2	8.42	-	T6H6	2.67	2.4
A8H2	6.74	-	C12H6	1.60	-
A10H2	11.64	21.7	T13H6	1.62	1.7
A14H2	10.70	-	T15H6	3.10	-
A17H2	4.52	-	C16H6	2.23	-
A19H2	8.51	-	T20H6	2.43	2.4
G1H8	1.64	-	T4H6	2.15	-
A3H8	2.15	2.3	T9H6	2.50	2.5
A5H8	2.20	2.6	T18H6	2.55	-
G7H8	2.50	2.6	C22H6	2.62	-
A10H8	2.05	2.3	T4M7	2.10	2.6
A14H8	2.36	2.2	T6M7	1.77	2.6
A17H8	2.38	-	T9M7	2.43	2.6
A19H8	2.03	2.6	T13M7	1.72	1.9
G21H8	2.26	-	T15M7	2.51	2.9
A8H8	2.14	2.3	T18M7	2.18	2.7
G11H8	2.70	-	T20M7	1.64	2.4

GLOBAL





## Reuse

We would not let a good thing go to waste.

By specializing in refurbished HP equipment,  
Global can outfit HP users with quality hardware  
and peripherals at a fraction of the new price.

## Renew

We can also help you efficiently market and  
dispose of your surplus or unused equipment with  
trade-in options and other programs, helping you  
get the maximum return.

## Global

We are a small minority-owned business.

Quality HP products at reduce cost.

And Great Service.

Call us at 800-736-8159.



Plotter

Printer

Workstation

Memory

# Save on Quality Equipment

713-890-1971

GLOBAL SOLUTIONS INC.

**BUY - SELL - LEASE HEWLETT PACKARD'S EQUIPMENT**

## Printers

HP 2225A-D ThinkJet ..... \$ 135  
(perfect for test equipment)

HP 2235A-D RuggedWriter .. \$ 595  
(support up to 6 multiple forms)

HP 3630A PaintJet ..... \$ 495  
(support continuous form feed color printing; great for data collecting; available with HP-IB interface)

HP C1645A PaintJet XL300 .. \$ 995  
(most affordable A-B Size color printer / plotter)

HP 33449A LaserJet 3 ..... \$ 795

HP LPM Printers ..... \$ Call

HP LaserJet 4V ..... \$ Call  
(great for A-B size laser quality output)

HP LaserJet 5si ..... \$ Call  
(24ppm; duplex option; support both A-B size media)

HP LaserJet Color ..... \$ Call  
(10ppm; support both A-B size media; color laser quality output)

### Service:

Hourly rate ..... \$ 65  
(LaserJet & DesignJet only)

*All products are refurbished unless otherwise stated. Prices are subjected to change and are based on availability.*

## Plotters

HP7550A A-B size 8-Pen ..... \$ 395  
(fastest pen plotter in the market; originally listed at \$3,695; support HPGL language)

HP7570A C-D size 8-Pen ..... \$ 1495  
(most affordable large size pen plotter)

HP7576A A-E size 8-Pen ..... \$ 1995

HP DesignJet 750C D/E size \$ Call  
(4min or less to complete color print-out; roll feed; 4M to 68M memory)

HP DesignJet 230 D/E size.. \$ Call  
(most affordable inkjet plotter)

HP DesignJet 250C D/E size \$ Call  
(most affordable color inkjet plotter)

Plotter Supplies ..... \$ Call

# 1-800-736-8159

*Warranty for refurbished equipment is 30 days. New equipment come with full manufacturer's warranty.*

## Workstations

System ..... \$ Call  
(HP 9000/700 Series)

HP 9000/825 server ..... \$ Call  
(complete system with DAT autoloader)

16Meg for HP 712 Sys ..... \$ 795  
(life time warranty)

HP 1GB SE SCSI2 drive ..... \$ Call

HP 2GB SE SCSI2 drive ..... \$ Call

HP 4GB 4mm DAT drive ..... \$ Call

## Classified

### 101 Want-to-Sell

Refurbished Compaq Contura 410CX 486DX2-50, 4Meg, 320M HD active color notebook. Like new condition. Price \$1,685 each. Quantity available.

### 102 Want-to-Buy

Looking to sell your excess or unused inventory? GSI is seeking to buy HP printers, plotters, workstations 9000/700 series. Please Call 713-890-1971.

## at a glance...

November '95

- Tony, sales ('87 University of Houston) - When Hakeem Alajuwon scored his 20,000<sup>th</sup> career point early this season 1995, it marked the second time a UH alumnus had achieved that milestone in the NBA. The first was Elvin Hayes. Clyde Drexler is also expected to reach that milestone by the end of this season. No other school has more than one alumnus that had achieved that mark.
- John, sales ('88 University of California at Berkeley) - Early preseason AP poll places California Golden Bears at 25<sup>th</sup> in the nation. Both recent former Cal players Jason Kidd of the Mavericks and Lamond Murray of the Clippers are doing well in the NBA with Kidd taking Rookie of the Year honor last year.

*This flyer is a monthly advertisement highlighting discount pricing to HP users. Products names reference herein are registered trademarks of their respective companies. For other products pricing and availability, please reach us at:*

**Global Solutions Inc.**  
18106 NW Freeway, #H8  
Houston, TX 77065  
713-890-1971 Tel  
713-890-2069 Fax





SCHOOL OF PHARMACY  
DEPARTMENT OF PHARMACEUTICAL CHEMISTRY

SAN FRANCISCO, CALIFORNIA 94143-0446  
FAX (415) 476-0688

Professor B. L. Shapiro  
966 Elsinore Court  
Pal Alto, CA 94303

(received 11/24/95)

### Correction for Intensities of Partially Relaxed NOESY Experiments

Dear Barry:

Obtaining interproton distances from NOESY spectra for structure studies is well established. As we have wished to obtain distances and bounds as accurately as possible, we have used much instrument time to generate (nearly) completely relaxed spectra, and we use a complete relaxation matrix approach (MARDIGRAS) to account for spin diffusion in our analysis of the spectral intensities. We have recently developed a way to analyze partially relaxed spectra, as shown below, which can save us much NMR acquisition time without the previous fear of skewing the resulting distances.

The integral of a NOESY cross peak  $I_{ij}$  is proportional to the longitudinal magnetization of spin  $j$ , i.e.,  $M_{zj}(0)$ , recovered before the pulses of next  $t_1$  incrementation. The relaxation delay is recommended as three times the longest  $T_1$  values. For short repetition time where  $M_{zj}(0)$  is smaller than 1, the intensities are scaled:

$$\begin{aligned} I_{ij} &= I_{0ij} M_{zj}(0) & (1) \\ \text{with } I_{0ij} &= [\exp(-Rt_m)]_{ij} & (2) \\ \text{and } M_{zj}(0) &= \sum [I - \exp(-R(rd + aq))]_{jk} & (3) \end{aligned}$$

where  $I_{0ij}$  is the intensity with full relaxation,  $R$  is the relaxation rate matrix,  $rd$  is the relaxation delay and  $aq$  is the acquisition time.

Cross relaxation rates (hence interproton distances) are determined with Eq. (2), which requires fully relaxed NOE intensities. Previous work on obtaining fully relaxed  $I_{0ij}$  from partially relaxed  $I_{ij}$  (M. Kock and C. Griesinger, *Angew. Chem. Int. Ed. Engl.* 1994, **33**, 332) relies on the assumption that the molecule is relatively small and  $T_1$ s of all spins can be measured. In this letter, we describe an approach that uses the ratio of NOE intensities above and below the diagonal to obtain  $I_{0ij}$ .

In general,  $I_{ij}$  does not equal  $I_{ji}$  if spin  $i$  and spin  $j$  relax at different rate. We consider  $M_{zj}(0)$  in Eq. (1) as a scaling factor, and it can be determined by the ratio:

$$M_{zi}(0) / M_{zj}(0) = I_{ij} / I_{ji} \quad (4)$$

We have developed a program that applies the above relation to a partially relaxed NOESY spectrum iteratively to obtain a set of  $M_{zi}(0)$ s that satisfy the following equations:

$$\begin{aligned} I_{0ij} &= I_{ij} / M_{zi}(0) & (5) \\ \text{and } I_{0ji} &= I_{ji} / M_{zj}(0) & (6) \\ \text{with } I_{0ij} &= I_{0ji} & (7) \end{aligned}$$

i.e., assuming the fully relaxed upper- and lower-diagonal intensities are equal. In another words, a partially relaxed NOESY matrix can be symmetrized by  $M_{zi}(0)$ s, which can be obtained by iteratively applying Eq. (4) to the upper- and lower-diagonal pairs of the NOE matrix. Once the  $M_{zi}(0)$ s are known, an estimation for  $T_1$ s is possible.

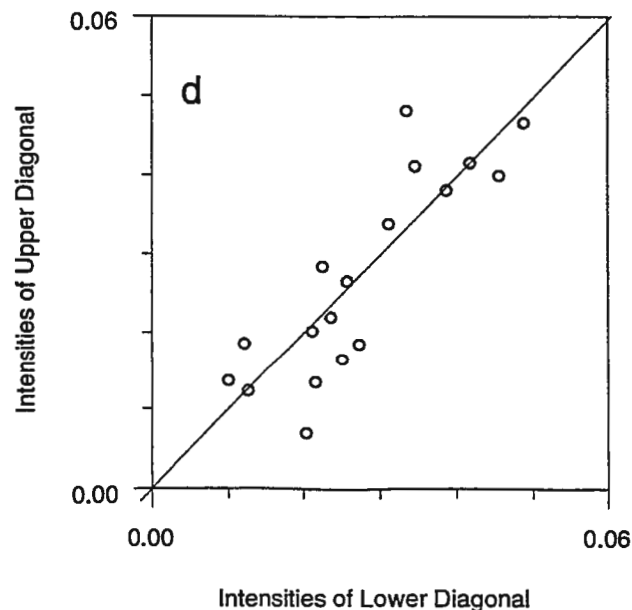
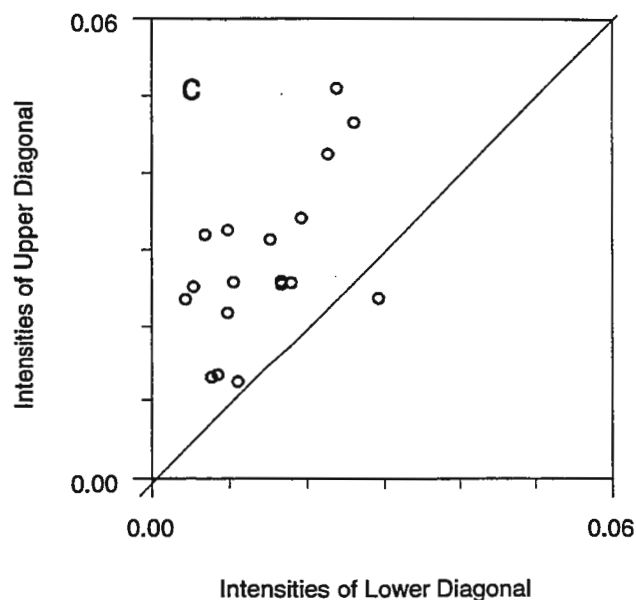
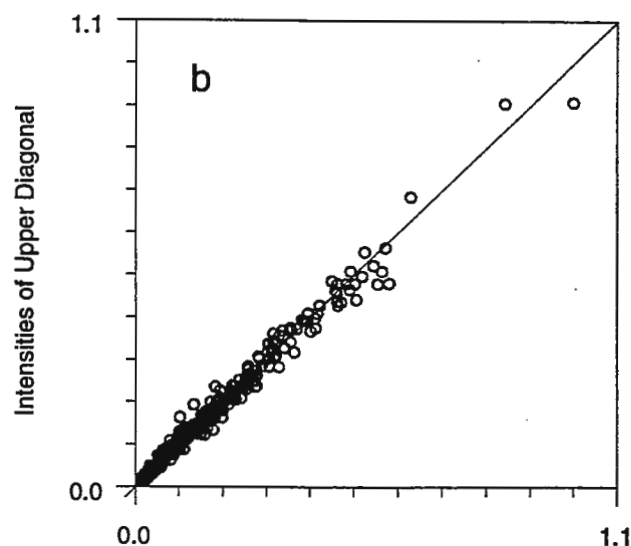
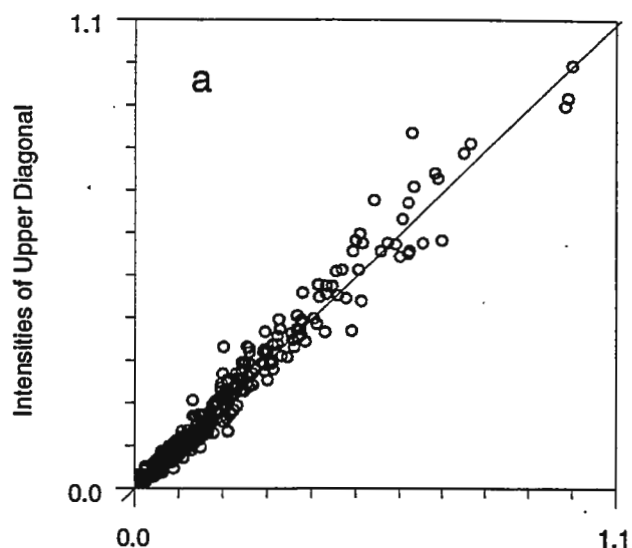
The method has been applied to a 270 ms NOESY spectrum of  $d(\text{GCATATGATAG})_2$  with 2.5 sec repetition. The circles plotted in Figure 1a are the upper diagonal intensities versus the lower diagonal intensities before the correction is applied. Figure 1b shows that after the correction the intensities are more symmetric. In Figure 1c, ADE H2 intensities are plotted. All the upper diagonal intensities (except one) are much stronger than the lower diagonal intensities. Figure 1d shows the intensities after correction.

The ratio of the upper- and lower-diagonal intensities may be affected by three factors: (1) partial relaxation; (2) experimental and integration errors; (3) different resolution for  $\omega_1$  and  $\omega_2$  axes. (1) and (3) yield systematic errors, i.e., peaks of each row are scaled by the same fraction. Point (2) errors are random and will be partially averaged by the summation in the iterations. The challenge to estimate  $T_1$ s is to separate  $M_{zj}(0)$ s from other systematic contributions. We assumed that for this particular data set, the effect of  $M_{zj}(0)$ s dominates the difference between upper and lower diagonal intensities. By assuming that  $M_{zj}(0) \approx 1 - \exp[-(rd + aq)/T_{1j}]$ , we obtained  $T_1$ s for all the protons. Table 1\* compares calculated and measured (by inversion-recovery)  $T_1$ s of H2, H6, H8 protons and THY methyl groups.

Sincerely,

*He Liu, Marco Tonelli, Thomas L. James*  
He Liu, Marco Tonelli, Thomas L. James

\* Continued on page 36



**Address all Newsletter  
correspondence to:**

Dr. B. L. Shapiro  
*The NMR Newsletter*  
966 Elsinore Court  
Palo Alto, CA 94303.

(415) 493-5971\* - *Please call  
only between 8:00 am and  
10:00 pm, Pacific Coast time.*

**Deadline Dates**

No. 449 (Feb.)	19 Jan. 1996
No. 450 (Mar.)	23 Feb. 1996
No. 451 (April)	22 Mar. 1996
No. 452 (May)	26 April 1996
No. 453 (June)	24 May 1996

\*Fax: (415) 493-1348, at any hour. Do not use fax for technical contributions to the Newsletter, for the received fax quality is very inadequate.

E-mail: 71441.600@compuserve.com.



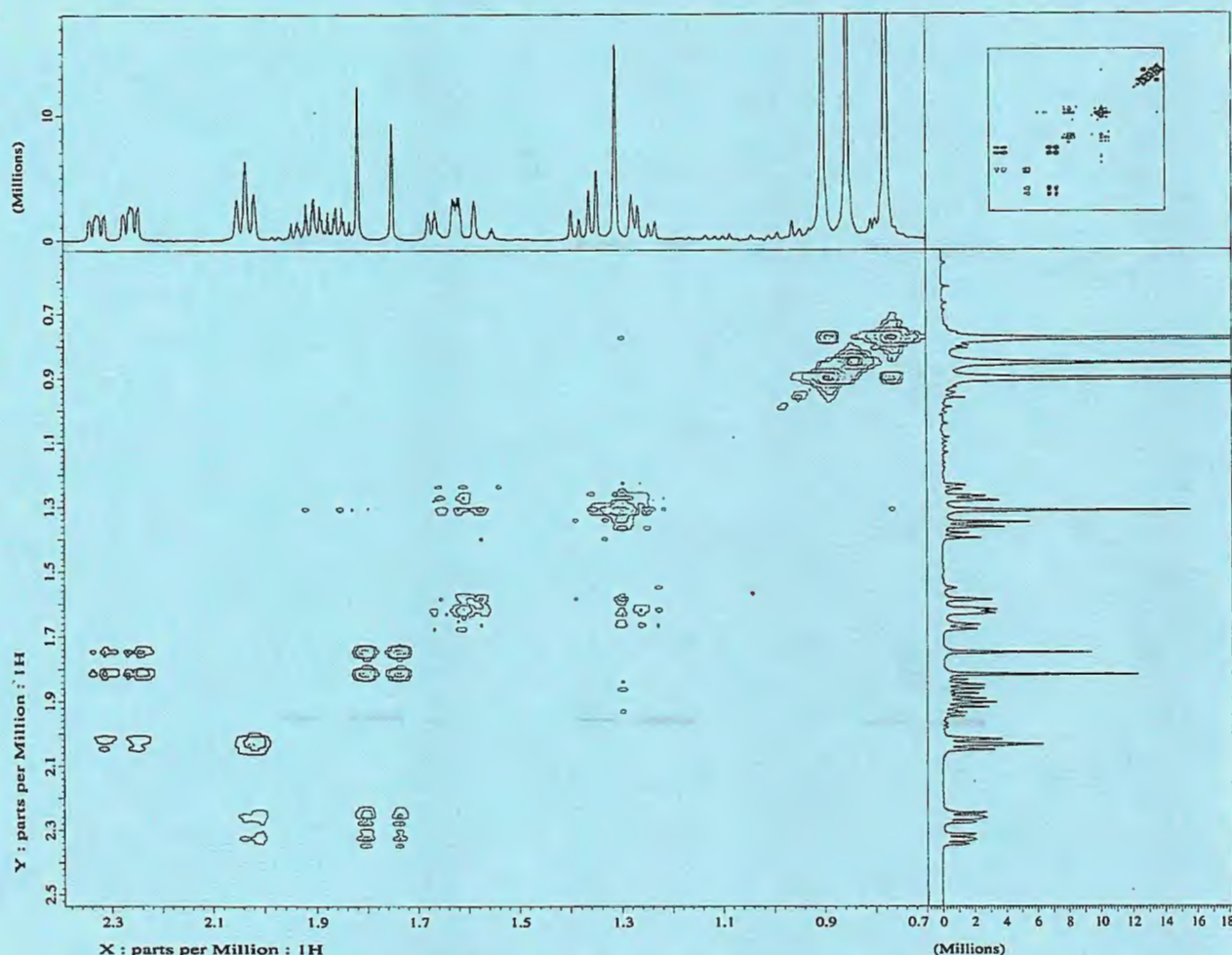
**The Newsletter's fiscal viability depends very heavily on the funds provided by our Advertisers and Sponsors. Please do whatever you can to let them know that their support is noted and appreciated.**

**Mailing Label Adornment: Is Your Dot Red ?**

If the mailing label on your envelope is adorned with a large **red dot**: this decoration means that you will not be mailed any more issues until a technical contribution has been received.



# ECLIPSE NMR Advantage: Gradient Enhanced 2D NMR Spectroscopy



*The Better Way!*

The ECLIPSE NMR Spectrometer from JEOL USA just increased your productivity. In less than one half of the 40 minutes usually required to complete the COSY, you can be back in your laboratory with proton, carbon and the COSY data. With JEOL's new low cost Matrix Gradients, this Double Quantum Filtered COSY

data was completed in less than 3 minutes. The ECLIPSE now expands the usual routine beyond the normal one dimensional proton survey spectrum to include the power of two dimensional NMR.

Now you can use the ECLIPSE NMR Advantage to your advantage.

JEOL USA, Inc.  
11 Dearborn Road  
Peabody, MA 01960  
Tel: 508/535-5900  
FAX: 508/536-2205  
EMAIL: [NMR@JEOL.COM](mailto:NMR@JEOL.COM)

**JEOL**  
Analytical Instruments Division  
MS • NMR • ESR